Review

Recent Advances in High-Performance Carbon-Based Electrodes for Zinc-Ion Hybrid Capacitors

Ying Liu [1,*], Lechun Song [1], Chenze Li [1], Caicheng Song [1] and Xiang Wu [2,*]

1   SINOPEC Dalian (Fushun) Research Institute of Petroleum and Petrochemicals, Dalian 116045, China; songlechun.fshy@sinopec.com (L.S.); lichenze.fshy@sinopec.com (C.L.); songcaicheng.fshy@sinopec.com (C.S.)
2   School of Materials Science and Engineering, Shenyang University of Technology, Shenyang 110870, China
*   Correspondence: liuying.fshy@sinopec.com (Y.L.); wuxiang05@sut.edu.cn (X.W.)

Abstract: Aqueous zinc-ion hybrid capacitors (ZIHCs) have emerged as a promising technology, showing superior energy and power densities, as well as enhanced safety, inexpensive and eco-friendly features. Although ZIHCs possess the advantages of both batteries and supercapacitors, their energy density is still unsatisfactory. Therefore, it is extremely crucial to develop reasonably matched electrode materials. Based on this challenge, a surge of studies has been conducted on the modification of carbon-based electrode materials. Herein, we first summarize the progress of the related research and elucidate the energy storage mechanism associated with carbon-based electrodes for ZIHCs. Then, we investigate the influence of the synthesis routes and modification strategies of the electrode materials on electrochemical stability. Finally, we summarize the current research challenges facing ZIHCs and predict potential future research pathways. In addition, we suggest key scientific questions to focus on and potential directions for further exploration.

Keywords: aqueous zinc-ion hybrid capacitors; carbon-based materials; cathode; energy storage device; electrochemical stability

1. Introduction

With the rapid changes in the energy patterns of the world, the efficient utilization and conversion of fossil fuels is an inevitable trend to achieve high-quality and sustainable energy development [1]. Recently, lithium-ion batteries (LIBs) have occupied a dominant position in the electronics industry, especially in portable electronics and electric vehicles [2]. However, limited Li resources and flammable organic electrolytes cause cost and safety concerns [3]. Thus, aqueous energy storage devices (metal-ion batteries, hybrid capacitors, and supercapacitors) have risen as potential solutions to the existing dilemma due to their high safety [4–9]. Among them, sodium and potassium ions possess ionic radii of 0.95 nm and 1.33 nm, respectively. It leads to slow diffusion kinetics and serious electrode polarization. In contrast, the ion radius of the zinc ion is relatively small (0.74 nm). Also, zinc anodes are characterized by their high theoretical capacity of 820 mAh g^{-1}, economical price, easy availability, and a low redox potential of −0.762 eV relative to the standard hydrogen electrode [10–12]. Nonetheless, the practical application of zinc anodes is limited by the scarcity of matching cathode materials and low power density [13–16]. Energy storage systems with high power densities and extremely long lifetimes can be fully recharged in a short period of time. They are also less susceptible to volume changes during cycling, which meets the needs of society for energy development. Zinc-ion hybrid capacitors (ZIHCs) incorporate their many benefits over traditional zinc-ion batteries. Generally, the device is featured by integrating the properties of a capacitive material with those of a battery-type material in a mild Zn-based electrolyte [17–21]. Due to the different operating potential ranges of these two types, the voltage of the matched device is extended.

As a result, there is an increase in the energy and power density of the devices. This is facilitated by the favorable combination of batteries and supercapacitors [22,23].

Since 2016, Wang and collaborators [24] have designed an aqueous zinc-ion capacitor assembled with oxidized carbon nanotubes and zinc metal as electrodes. It can be repeatedly charged and discharged for 5000 cycles (10 mV s^{-1}) with the working voltage of 0–1.8 V. Then, Kang et al. [25] reported the study of aqueous activated carbon (AC)/Zn capacitors with ultra-long lifetimes. ZIHCs are rapidly growing as a research hotspot [26]. Further, Kang's group [27] constructed a hybrid ion capacitor with MnO_2 and AC as cathode and anode, respectively. The device with Zn^{2+} aqueous solution as electrolyte can output a maximum power density of 13 kW kg^{-1}. During the past decade, carbon-based materials have been exploited as cathode materials owing to their high conductivity and customizable pore structure, including biomass and polymer-derived carbon, metal organic compounds derived carbon, graphene, and carbon nanotubes [28–30]. For example, Alshareef's group [31] prepared hybrid capacitors with oxygen-enriched porous carbon cathodes and carbon-coated zinc anodes. Benefiting from the EDLC of the porous carbon and the pseudocapacitance provided by the oxygen functional groups, the assembled ZIHCs obtain a specific capacity of 179.8 mAh g^{-1}. The energy density is up to 104.8 Wh kg^{-1} (0.1 A g^{-1}) with a voltage window of 0–1.9 V. Fan and co-workers [32] designed honeycomb porous carbon using polyacrylonitrile (PAN) as a precursor through a pre-oxidation and activation process. This abundant pore and interconnected structure facilitate rapid charge transfer and generate numerous ion adsorption sites. The assembled capacitor shows a specific capacity of 238 mAh g^{-1} at 0.1 A g^{-1}. Furthermore, it achieves an energy density of 193.6 Wh kg^{-1}, corresponding to a power density of 76.6 W kg^{-1}. Li et al. [33] fabricated porous carbon rich in pyridine nitrogen (PrN) with Zn and Co bimetallic organic skeletons as precursors. The content of PrN can be controlled to 56% by changing the annealing temperature. This high pyridine N content provides rich reaction sites for the structure of materials. Moreover, the presence of residual cobalt nanoparticles contributes to accelerating electron transfer. Based on this, the assembled ZIHCs deliver a specific capacity of 302 mAh g^{-1} (1 A g^{-1}) and an energy density of 157.6 Wh kg^{-1}.

The energy density of these reported devices is significantly weaker than expected. It can be ascribed to the distinct energy storage mechanisms of these two electrodes. This leads to the dynamic imbalance of ZIHCs, which fails to acquire high energy and power density [34]. This asymmetric device tends to increase the overpotentials of hydrogen and oxygen evolution in aqueous solutions. Its voltage range is generally restricted to 2.0 V [35,36]. Nevertheless, the energy density of aqueous ZIHCs is still far below that of batteries. Therefore, the charge storage capacity and voltage window can be increased by designing the electrode structure, electrolyte, and electrode/electrolyte interface [37].

Herein, we focus on the recent developments of carbon-based materials as electrodes for aqueous ZIHCs. First, we distinguish the different types of ZIHCs according to the properties of electrode materials. Then, we discuss the structure and morphology of carbon-based materials. Their cycling, rate performance, and durability are demonstrated when they are assembled as positive electrodes into capacitors. Further, we highlight the modification strategies of carbon-based materials, including surface modification, morphology and size tuning, and heterogeneous atom doping. We also summarize the energy storage mechanism in conjunction with the electrode structural changes. Finally, we present a conclusion and prospect the future development of ZIHCs.

2. The Bases of Zinc-Ion Capacitors

2.1. The Growth of Energy Storage Technologies

Among the various energy storage systems, supercapacitors and batteries are two highly representative electrochemical energy storage technologies. The former is a promising device with the merits of rapid charge capabilities, longevity, and excellent power density. The latter demonstrates high energy density and voltage window. Research on energy storage devices began in the 1800s (Figure 1). H. I. Becker first discovered elec-

trochemical capacitors with a high farad in 1954. In the following 20 years, Whittingham reported reversible electrochemical embedding reactions of layered TiS_2 with lithium in Li/TiS_2 batteries [38]. However, Li/TiS_2 batteries cannot be developed into commercially promising secondary batteries. It can be attributed to the low open-circuit voltage of the TiS_2 cathode (2.2 V). Goodenough et al. [39] proposed that the layered $LiCoO_2$ materials can be used as the cathodes for LIBs. It presents an open-circuit voltage of 4.0 V, almost twice that of the TiS_2 electrode. In the 21st century, research on various metal-ion capacitors has also become increasingly attractive with the massive growth in energy demand [40].
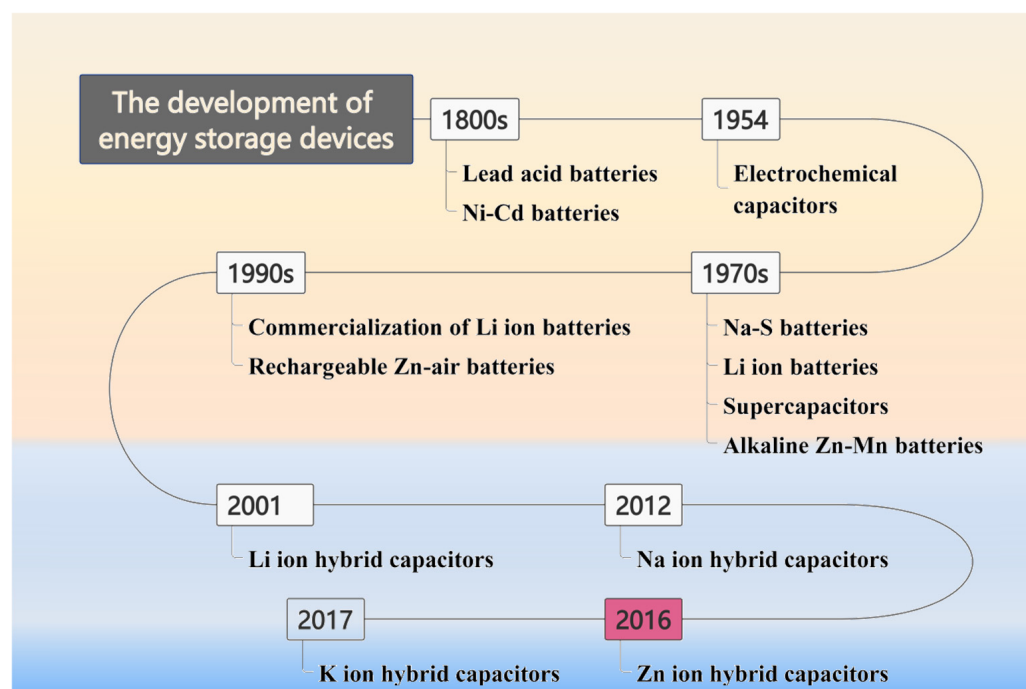

Figure 1. The growth of energy storage technologies.

Supercapacitors are mainly employed in portable electronic devices, rail public transportation, heavy trucks, and backup energy for uninterruptible power supply (UPS) [41]. Based on the principles of charge accumulation, the cathode can be categorized into two main types: double electric layer capacitors (EDLCs) and faradaic electrode materials [42,43]. The former involves the formation of a double layer by electrostatic adsorption of charges at the electrode/electrolyte interface. The latter represents a prompt reversible redox process occurring on/near the surface. The difference between the two is that EDLC is not undergoing a faradaic process [44,45]. The electrode materials for supercapacitors include carbonaceous materials, conducting polymers, and transition metal oxides and hydroxides [46–49]. Notably, carbon-based materials are characterized by abundant resources, inexpensiveness, extensive specific surface area, and superior electrical conductivity [50,51]. During the past few years, a multitude of studies have concentrated on the design of the pore structure of such electrodes to modulate the electrochemical performance of the devices [52]. Liu et al. [53] designed an activated porous carbon material with a specific surface area of 843 $m^2\ g^{-1}$ via rapid high-temperature shock carbonization and the HTS-KOH activation approach. The prepared electrodes are assembled into supercapacitors with an energy density of 25 Wh kg^{-1} and a power density of 582 W kg^{-1}. Prabakar's group [54] synthesized activated carbon nanosheets with a specific surface area up to 2943 $m^2\ g^{-1}$ by one-step activation method. The assembled symmetric supercapacitor achieves a capacitance of 403 F g^{-1} with an energy density of 32.9 Wh kg^{-1} (0.5 A g^{-1}).

2.2. The Types of ZIHCs

Benefiting from the synergistic strengths of supercapacitors and batteries, the novel ZIHCs are regarded as critical candidates for energy storage technologies. This is attributed to their ability to satisfy market requirements for high energy and power density [55]. Among them, electrodes can be divided into capacitor-type and battery-type materials. The former is mainly carbon-based electrodes (derived carbon and graphene-based materials) and pseudocapacitive electrodes (MXene and polymer–carbon materials) [56]. Generally, zinc ion adsorption/desorption reactions occur on their surfaces during charging and discharging. The latter is generally metallic zinc, Mn, and V oxides, which mainly occur in zinc ion insertion/extraction reactions. Based on the unique characteristics of carbon-based electrodes, the cathode and anode materials of ZIHCs can be classified into carbon materials/Zn foils and manganese-based or vanadium-based oxides/carbon materials.

Figure 2 illustrates the dual energy storage mechanisms of ZIHCs. From Figure 2a, carbon-based cathodes utilize the EDLC mechanism to facilitate highly reversible ion adsorption/desorption processes, thus providing excellent power densities. In fact, their total capacitance is contributed by EDLC and pseudocapacitance. Therefore, a redox reaction can occur on the surface or near the surface of a carbon electrode. On the anode side, zinc ions in the electrolyte can be deposited and stripped on the zinc foil with the charging and discharging process to obtain excellent energy density.
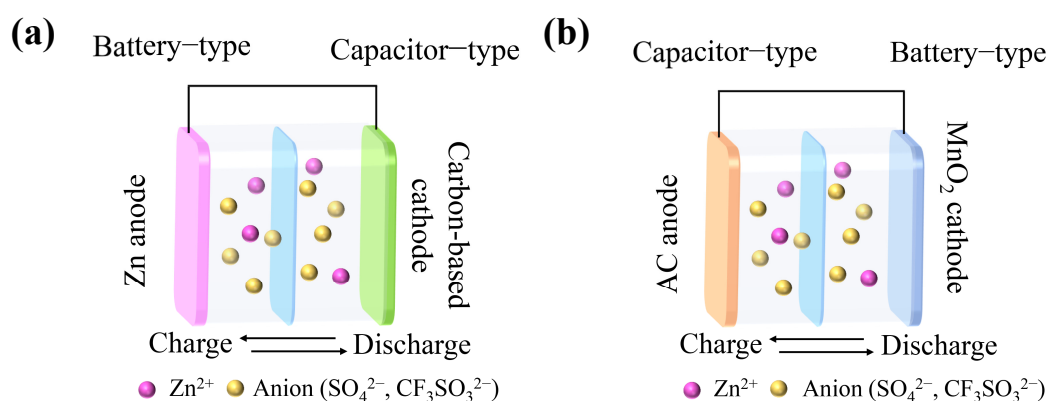

Figure 2. The energy storage mechanism of different electrodes. (**a**) Carbon-based cathode/Zn anode capacitor. (**b**) MnO$_2$ cathode/AC anode capacitor.

In Figure 2b, a Mn-based oxide/carbon material hybrid capacitor is taken as an example. When charging, zinc ions escape from the battery-type cathode and adhere to the surface of the capacitor-type anode. In the discharge phase, zinc ions are desorbed from the anode and embedded in the structure of the cathode. This reversible transfer of zinc ions contributes to the stable electrochemical performance of ZIHCs.

Compared with the two systems, the capacitive material as the cathode can provide rapid ion adsorption/desorption, thus achieving high power density. However, zinc anode is prone to producing zinc dendrites, which leads to potential safety hazards. The battery material as cathode enables a dendrite-free system. The voltage range of the device can be extended up to 2 V, showing high energy density. However, their electrochemical performance suffers from issues such as low rate capability and cycling stability, which are attributed to the dissolution of the cathode material.

3. Carbon-Based Electrode Materials

Carbon is an indispensable material to promote social development and progress. In the last two decades, carbon materials with various allotropic structures (graphene, diamond, carbon fiber, and carbon nanotubes) have grown rapidly in a wide range of fields. In particular, they stand out in new energy sources owing to their highly theoretically specific surface area and superior electrical conductivity [57]. From Figure 3, carbon-based

cathodes mainly include commercial activated carbon (AC), biomass or polymer-derived carbon, metallic organic compound-derived carbon, nanofibers, and other graphite-like carbon materials. This section mainly introduces the structure and morphology of these carbon materials and their corresponding electrochemical performance.
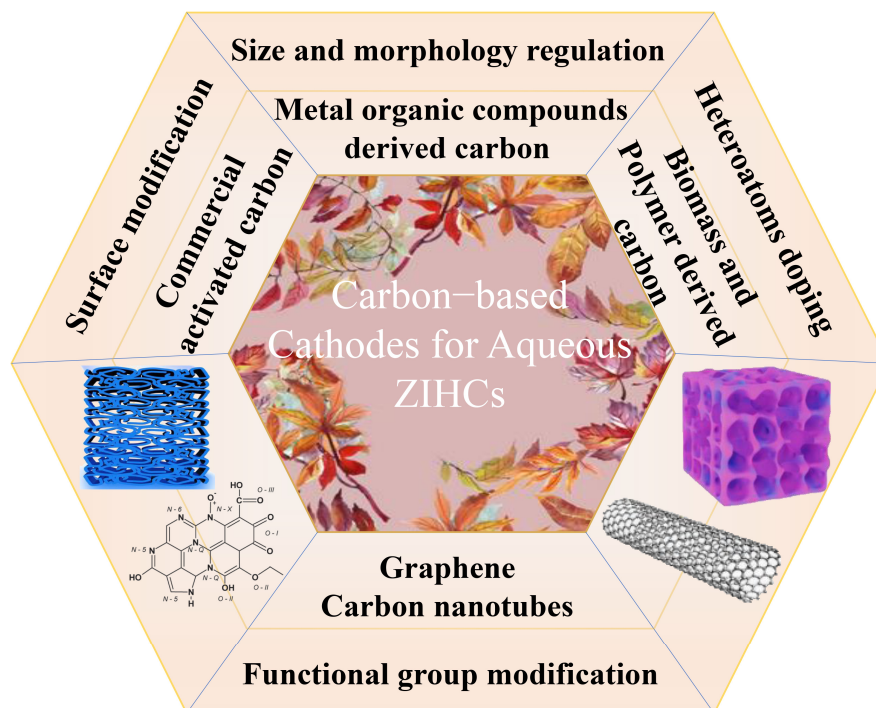

Figure 3. Classification and synthetic approaches of carbon-based cathodes for aqueous ZIHCs.

3.1. Amorphous Carbon Materials

3.1.1. Commercial Activated Carbon

In recent years, AC has attracted great interest as a promising candidate electrode material for ZIHCs because of its specific surface area of 3000 m^2 g^{-1}, rich pore structure, high chemical stability, and wide working potential window. They can usually be prepared from various precursors such as polymers, biomass, coal, organometallic frameworks, and organic salts. However, commercial AC has a specific capacity of only 100–200 mAh g^{-1}. The electrochemical performance of ZIHCs depends on the pore structure, conductivity, and surface properties of carbon-based electrodes. Pore structure is critical for charge storage and diffusion of hydrated Zn^{2+} ions [58]. Strategic designs of pore structures (including pore volume, size distribution, and surface functional group chemistry) are effective approaches to enhance the specific capacitance of electrodes.

Pore size distribution is an important parameter affecting zinc-ion storage. The pore structures in AC are usually categorized into micropores with a size less than 2 nm, mesopores with a size of 2–50 nm, and macropores with a size over 50 nm [59–61]. However, not all pores in the material are beneficial to charge storage. Both micropores and mesopores contribute to the EDLC. However, a part of the micropores prevents the embedding of electrolyte ions because of the distorted pore channel or small pore size. It also deprives their electrochemical activity at high loadings. The solvated $[Zn(H_2O)_6]^{2+}$ and SO_4^{2-} are the main carriers in the charging and discharging process of ZIHCs [62]. Its ion diameters are 0.86 and 0.59 nm, respectively. After solvation, the radius of Zn^{2+} is increased compared with the original one. For carbonaceous materials with pore sizes less than 1 nm, most of the solvated Zn^{2+} ions are limited by the pore structure. This leads to their inability to provide capacitive contributions.

From Figure 4, when there are various pores in the structure of carbon materials, they are prone to diffuse in the one with large pore size. It contributes to enhancing the specific

capacitance of the devices. The pore size structure affects the ion diffusion resistance of the electrode. Small pore size enhances the diffusion resistance of electrolyte ions. The presence of mesopores and macropores can shorten the ion migration path and contribute to the rate capacity [63]. Zhang and colleagues [64] systematically compared various samples with similar specific surface areas but distinct pore structures. It is found that the materials with abundant micropore structure (0.6 nm) are generally lower in capacitance and rate performance than those with mesoporous channels. This phenomenon is associated with the partial failure of the microporous structure, which hinders the accommodation and storage of hydrated zinc ions. Hence, it is the key to stabilizing the cycle performance to match the appropriate pore channels.
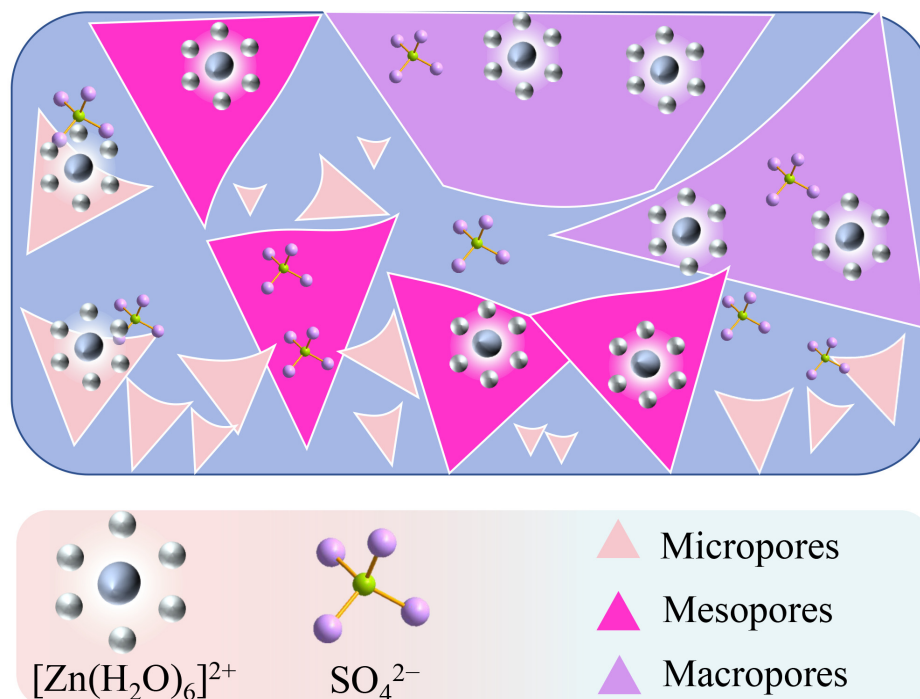

Figure 4. Schematic of charge carriers embedded in various pore structures.

To address the issue of the low specific capacitance of commercial AC, researchers have made many efforts. Dong et al. [25] designed the AC/Zn devices with a capacity of 121 mAh g^{-1} and an energy density of 84 Wh kg^{-1}. In fact, there is still space for improvement in cycle performance. Surface-functionalized AC with reasonable pore size enhances chemical binding with carriers, which contributes to an increase in specific capacity [65]. For instance, An's group [66] prepared the AC material with a mesoporous structure by polymerization PVP dehydrogenation process. This increases the number of oxygen groups on the surface of AC. The modified materials, such as cathodes, show an abundance of electrochemical active sites and rapid ion diffusion and transmission ability. Therefore, the assembled ZIHCs can still deliver a specific capacity of 72 mAh g^{-1} even at a current density of 10 A g^{-1}. In addition, the cycle life can reach 40,000 cycles with a capacity retention rate of 78% (Figure 5a).

The specific capacity of AC electrodes is enhanced based on surface modulation techniques, but there are limited improvements in their conductivity, wettability of the electrode and electrolyte surfaces, and specific surface area. Therefore, researchers have developed some effective modification strategies and superior electrode materials. Heterogeneous atom doping can introduce O-/N-containing functional groups. This offers fast redox reactions for the electrodes and increases the pseudocapacitive contribution to charge storage [67,68]. The construction of novel nanostructures or hierarchically porous carbon materials can effectively increase the adsorption sites. This accelerates ion/electron

transport and favors the rate capacity [69]. Further detailed discussions are presented in the subsequent sections.

3.1.2. Metal–Organic Compound Derived Carbon

Metal–organic compounds are converted into nanostructured carbon materials through high-temperature calcination or controlled chemical reactions. This conversion process is conducive to the formation of porous architecture. This hierarchical porous structure facilitates the optimization of electrochemical performance. Zhang and collaborators [70] fabricated ultra-thin layered porous carbon nanoplates (Ca-900 samples) using calcium gluconate precursor by in situ template method. The tuning of calcination temperature can optimize the specific surface area and porosity of carbon materials. The assembled device shows an energy density of 75.22 Wh kg^{-1} and a power density of 879.12 W kg^{-1}. After 4000 times of charge and discharge, the capacitance retention rate is 90.9%.

Metal–organic frameworks (MOFs) constitute a class of crystalline compounds synthesized by coordination of metal ions with organic linkers. MOF-derived carbon materials can possess a wide range of specific surface areas and rich porous structures by high-temperature calcination and etching processes [71]. Li et al. [72] designed a rod-like porous carbon fabricated by pyrolysis of MOF (MIL-88B). Based on the structural features of MOF and the synergistic effect of alkali activation, the carbon rod material possesses a specific surface area (SSA) of 1272.4 m^2 g^{-1}. The assembled device can still show a specific capacity of 73.5 mAh g^{-1} at 50 A g^{-1}. The capacity retention of 96.5% (10 A g^{-1}) is achieved after 10,000 cycles. Our group [20] prepared V metal–organic framework (MOF)-derived porous carbon anodes. The assembled devices present specific capacities of 168 and 140 mAh g^{-1} with a capacity loss of 16.7% at 0.1 and 2 A g^{-1}, respectively. These kinds of materials are often treated by strong acid/alkali etching, which increases the technical difficulty and cost. Therefore, there is an urgent need to design eco-friendly, high-performance carbonaceous materials.

3.1.3. Polymer-Derived Porous Carbon

Polymers are complex structures composed of many macromolecular chains. They possess nanoscale self-assembly ability. Compared with small molecular hydrocarbons, polymers as carbon sources show controllability in structure and doping amount. A variety of porous carbonaceous structures, including spherical particles, fibrous materials, films, or membrane-type materials, can be prepared by matching suitable polymer precursors, such as polyacrylonitrile, polyphenylamine, and conjugated polymers. Due to the unique atomic composition of polymer precursors, non-metallic atoms can be doped by pyrolysis, including N, B, P, and S. These types of atoms are combined into the carbon framework individually or jointly to optimize the energy storage capability of carbon materials [73]. Yang et al. [74] developed a hierarchical porous carbon fiber derived from polyvinylpyrrolidone/polyacrylonitrile (PVP/PAN) by electrospinning. The device assembled with PVP-/PAN-derived porous carbon fibers shows a specific capacity of 208 mAh g^{-1} and a rate retention of 49.5% (0.5~5 A g^{-1}). After 10,000 stable cycles, the capacity maintains 72.25% of the initial capacity. This multi-channel structure is beneficial to the specific capacity and rate performance of ZIHCs. However, the specific surface area obtained by this direct pyrolysis is only 449.05 m^2 g^{-1}. Therefore, its cyclic stability is limited. Liu group's [75] studied the pyrolysis of chitosan aerogels to produce porous carbon with 3D honeycomb lattice. The combination of nitrogen and oxygen realizes the co-doping of carbon materials. However, the specific surface area of carbonized chitosan is only 1000 m^2 g^{-1}, and it lacks essential micropores and mesopores. Combined with the KOH activation strategy, its specific surface area can be increased to 2267 m^2 g^{-1}. Therefore, the capacity retention of the assembled device can remain at 86.3% after 10,000 cycles.

Carbon materials derived from asphalt have garnered extensive research attention for their applications in supercapacitors and LIBs [76–78]. However, the activation of asphalt with complex compositions at high temperatures usually leads to violent volatilizing

of light components and polymerization of polycyclic aromatic hydrocarbons [79]. To regulate the pore size during fabrication, Liu and co-workers [80] proposed two steps of carbonization and alkali activation to enhance its structural stability. In Figure 5b, compared with commercial AC, the specific surface area of this material can be increased to 3525 m^2 g^{-1}. The porous structure is composed of micropores and abundant mesopores, which effectively increase the ion occupation sites. The fabricated device achieves a specific capacity of 172.7 mAh g^{-1} at 1 A g^{-1}, and it retains a capacity of 119.4 mAh g^{-1} at 20 A g^{-1} (Figure 5c). Lu and collaborators [81] designed an N-doped asphalt-derived carbon material (NPC) as a cathode. In Figure 5d, incorporating N into the carbon electrode material enhances its electrical conductivity, and the addition of pyridine N effectively increases the electrochemical kinetics. They further proposed a nitrogen redox mechanism. From Figure 5e, the activation energy (E$_a$2) of the NPC electrode is much superior to that of PC one. This indicates that the addition of N triggers multiple redox processes in favor of increasing the pseudocapacitance. The assembled device possesses a capacity of 136.2 mAh g^{-1}. When the current density increases from 0.3 A g^{-1} to 15 A g^{-1}, the capacity retention rate is 50.8% (Figure 5f). In addition, it only experienced 4.6% self-discharge capacity loss within 24 h.
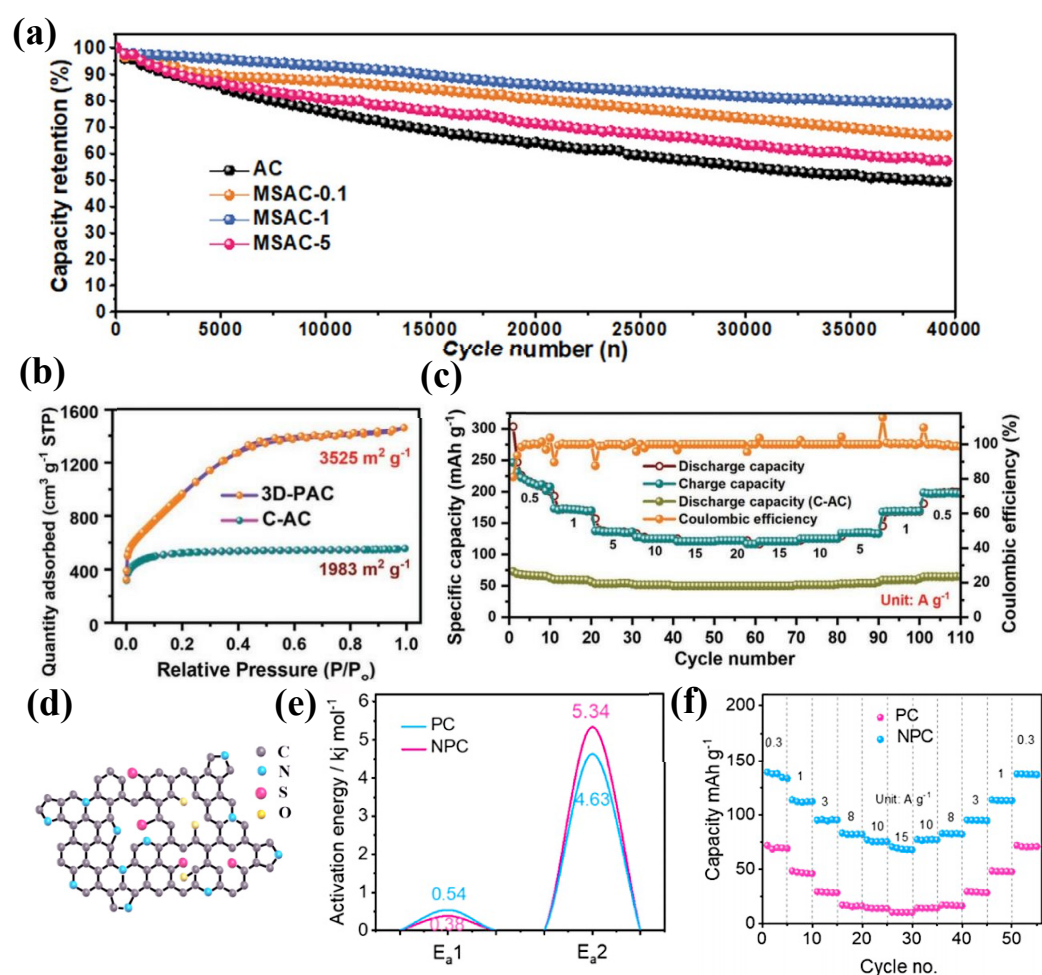

Figure 5. Effect of specific surface area on electrochemical performance of materials (**a**) The capacity retention (10.0 A g^{-1}) for the various electrodes. Reproduced with permission [66], Copyright 2020, Elsevier B.V. (**b**) Nitrogen adsorption–desorption isotherms of the two materials. (**c**) Rate capability of the assembled device. Reproduced with permission [80], Copyright 2020, Wiley-VCH GmbH. (**d**) Schematic structure of NPC. (**e**) The activation energy comparison of PC and NPC. (**f**) Rate performance. Reproduced with permission [81], Copyright 2021, American Chemical Society.

3.1.4. Biomass-Derived Porous Carbon

Biomass-derived porous carbon materials are frequently applied as cathodes for capacitors due to their cost-effectiveness, structural diversity, and preparation convenience [82]. Li and co-workers [83] synthesized pencil shaving-derived carbon materials and obtained optimal PSC-A600 electrodes by adjusting the pyrolysis temperature. This porous structure enables a fast ion transport rate and provides sufficient charge storage space. Therefore, the Zn/PSC-A600 device presents a specific capacity of 183.7 mAh g^{-1}. From Figure 6a, it can perform 10,000 cycles at 10 A g^{-1} and maintain a retention rate of 92.2%. Qiu's group [84] prepared porous carbon positive electrodes (LHPCs) by the self-templating method employing lignin as a carbon precursor. The electrode material demonstrates fast electrochemical kinetic processes. This is due to the rich pore structure and the introduction of carboxyl functional groups. The assembled Zn/LHPCs capacitors obtain an energy density of 135 Wh kg^{-1} at a power density of 101 W kg^{-1}.

However, the impurities and functional groups of biomass carbon-based raw materials accelerate the self-discharge speed of the assembled hybrid capacitor. This is closely related to the pore structure of the carbon cathode. This pore effect exacerbates charge redistribution and carbon oxidation [85]. Li et al. [86] synthesized oxygen-enriched multistage porous carbon by olive pyrolysis through chemical activation. Oxygen-enriched functional groups provide additional capacitance and boost the wettability and conductivity of porous carbon. The as-built devices obtain an energy density of 136.3 Wh kg^{-1} and a self-discharge rate of 2.3 mV h^{-1} (Figure 6b). They can achieve 20,000 charge and discharge cycles at 10 A g^{-1} (Figure 6c).
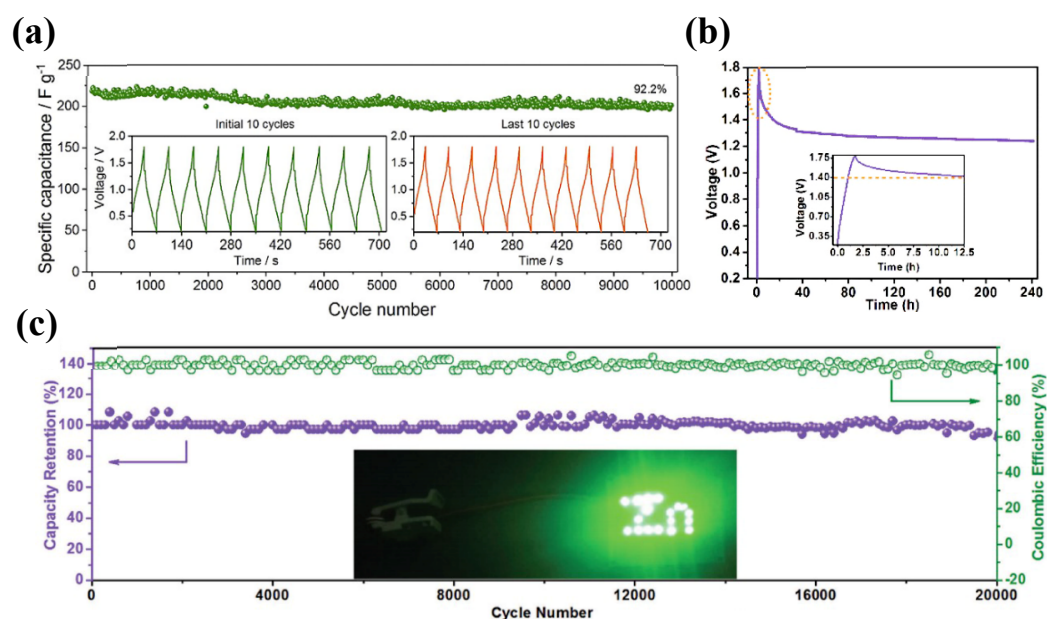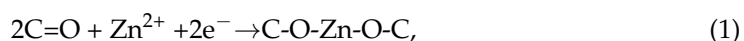

Figure 6. The cycle capability of biomass-derived porous carbon. (**a**) Cycle performance. Reproduced with permission [83], Copyright 2020, Elsevier B.V. (**b**) Self-discharge curves. (**c**) Cycling durability at 10 A g^{-1}. Reproduced with permission [86], Copyright 2023, Wiley-VCH GmbH.

3.2. Carbon Nanofibers

Flexible wearable devices have been a hot research topic. Therefore, there is a demand for the exploitation of flexibility electrodes. Typically, the fabrication of electrodes depends on the support of current collectors and additives in addition to active materials, which can reduce the total energy density. One-dimensional (1D) carbon nanofibers are highly promising for the construction of freestanding cathodes, which is attributed to their favorable flexibility and abundant pore structure. However, their hydrophobicity hinders charge transport at the electrolyte–electrode interface, demonstrating a large interfacial resistance.

Surface modification improves the hydrophilicity of carbon-based materials. For instance, this is a viable approach to enhance the chemisorption of metal ions on electrode materials. Zhang and collaborators [87] synthesized flexible oxygen-enriched carbon fiber films by electrostatic spinning and acid-assisted oxidation. ZIHCs with this carbon fiber cathode show an energy density of 97.7 Wh kg^{-1} and a power density of 9.9 kW kg^{-1}. Also, they maintain long-term cycling stability (81%) of 50,000 cycles. Figure 7a demonstrates the near-zero superhydrophilicity angle. It reduces the interfacial resistance between electrolyte and electrode. The adsorption of zinc ions on the electrode surface is greatly enhanced. Density functional theory (DFT) calculations show the chemisorption relationship between zinc ions and C=O functional groups (Figure 7b). Among them, zinc ions are more easily adsorbed between two carbonyl groups. The adsorption process is shown below:

$$2C=O + Zn^{2+} + 2e^- \rightarrow C\text{-}O\text{-}Zn\text{-}O\text{-}C, \tag{1}$$

The existence of oxygen-enriched functional groups significantly improves the wettability of carbon fiber and promotes the chemisorption of zinc ions. In addition, these cathodes could operate stably with a loading of 20 mg cm^{-2} and 180° bending. Their specific capacity decreases by 19% (5 A g^{-1}) after 50,000 cycles (Figure 7c).

Figure 7. Wetting behavior and cycling stability. (**a**) Contact angles. (**b**) DFT calculations for zinc storage behavior. Red, brown, white and gray balls represent oxygen, carbon, hydrogen and zinc atoms, respectively. The regions indicate the increase (yellow) and decrease (blue) of electron density. (**c**) Long-term cycle at 5 A g^{-1}. The pink and orange curves represent capacity and coulombic efficiency, respectively. Reproduced with permission [87], Copyright 2021, Elsevier B.V.

3.3. Graphite-Type Carbon Materials

This refers to a high-performance material with a graphite-like microcrystalline structure. Representative members include graphene, carbon nanotubes, and carbon fibers [24,88]. These materials are characterized by a layered accumulation of carbon atoms interconnected by van der Waals interactions. This unique layered structure endows graphite-like carbon materials with favorable electrical and thermal properties, as well as excellent chemical stability. Therefore, they show wide application potential in various fields, including energy storage, electronic devices, composite materials, and catalytic technology [89].

3.3.1. Carbon Nanotubes

One-dimensional carbon nanotube (CNT) materials offer unique fast carrier transfer pathways, but the limited specific surface area (less than 500 $m^2 \, g^{-1}$) hinders their further development. Previous studies have demonstrated that the introduction of pseudocapacitive active sites on carbon nanotubes can increase the specific capacitance of carbon nanotubes [24,90,91]. Wang's group [24] used oxidized CNT (oCNT) as cathode and revealed the role of oxygen groups in ion storage by electrochemical characterization. As shown in Figure 8a, Zn^{2+} on the oxygen-containing groups of the oCNT electrode undergoes electrochemical adsorption/desorption. The surface-endowed ZICs are confirmed to provide better performance than the pure carbon nanotube cathode.

3.3.2. Graphene

Graphene, featuring a single atom thickness, superior electrical conductivity (10^6 S cm^{-1}), mechanical properties, and a specific surface area of 2630 $m^2 \, g^{-1}$, is a suitable positive material for ZIHCs. However, two-dimensional (2D) graphene tends to aggregate. Moreover, there are morphological defects such as holes, edges, cracks, and heteroatoms on the surface of graphene [92]. This greatly limits its properties. Three-dimensional (3D) graphene is a novel class of carbon nanomaterial composed of 2D graphene on a macroscopic scale. When graphene nanosheets are interconnected as building blocks, they can be assembled into 3D structures from the bottom up. Han et al. [93] fabricated a ZIHC based on 3D nanostructures graphene and polyaniline composites as cathodes (Figure 8b). It shows an energy density of 205 Wh kg^{-1} (0.1 A g^{-1}). From Figure 8c, it can still maintain 80.5% of the initial capacity after 6000 cycles of repeated charging and discharging. However, these high-porosity materials always present low bulk density and high weight capacitance. It reduces the volume capacitance and hinders the practical application of the device [88]. Therefore, it is very necessary to develop highly dense structures. Zheng's group [94] prepared a high-density nanoparticle 3D porous graphene (3D-PG-1) through capillary evaporation. The pores formed through the evaporation process provide extensive pathways for the rapid diffusion of Zn^{2+}. It also weakens the strong electrostatic force of Zn^{2+} embedded in the structure. This ensures that the electrode achieves 30,000 stable cycles (Figure 8d).

Recently, graphene-derived 3D network/aerogel structures have been identified to enhance the number of active sites in electrode materials. Compared with conventional graphene films, graphene aerogels feature stable 3D networks and high pore volumes [95]. Okhay et al. [96] synthesized reduced graphene oxide aerogels with optimal properties by tuning the freeze-drying conditions. The graphene oxide composite electrode demonstrates favorable uniformity and surface wettability with a specific capacitance of 129 F g^{-1} at 0.1 A g^{-1}.
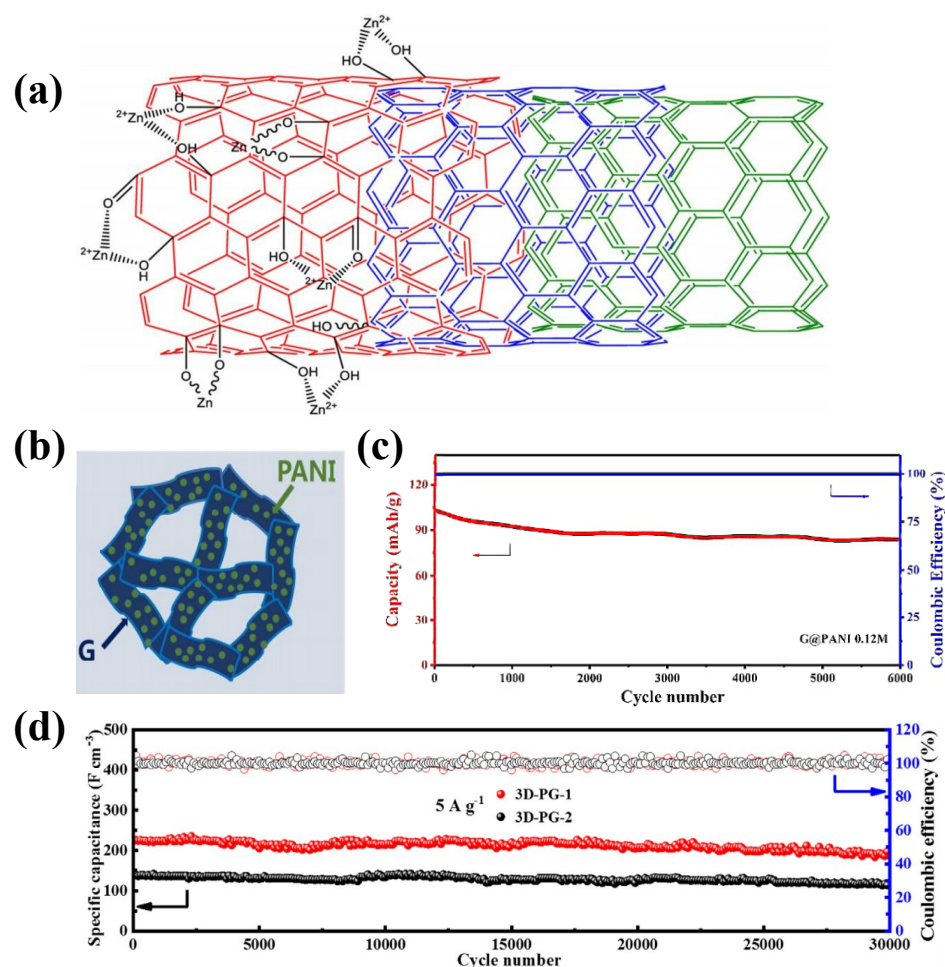
Figure 8. The electrochemical performance of the other carbon electrodes. (**a**) Schematic of zinc ion adsorption on the surface of oCNTs electrode, Reproduced with permission [24], Copyright 2016, Frontiers. (**b**) 3D cross-linked structure of graphene@PANI materials (**c**) The cycle stability of graphene@PANI electrode at 5 A g^{-1}. Reproduced with permission [93], Copyright 2018, Royal Society of Chemistry. (**d**) Long cycle stability at 5 A g^{-1}. Reproduced with permission [94], Copyright 2021, Elsevier Ltd.

4. Modification Strategies

These carbon materials suffer from many issues as electrode materials, including structural instability, poor wettability, and slow electrochemical kinetic. This hinders efficient carrier transport. Therefore, it is essential to modify the carbon-based materials to mitigate these adverse effects. Researchers have proposed several effective strategies, including surface modification, morphology and size tuning, and heterogeneous atom doping.

4.1. Surface Modification

To further improve the cycle stability, it is a feasible method to construct novel carbon-based composites. Xin et al. [97] prepared a poly(4,40-thiodiphenol, TDP)-modified nanoporous AC cathode material. The introduction of this polymer increases the capacitance contribution and broadens the voltage window to 1.9 V through the faraday process. The areal energy density of the device is 1.03 mWh cm^{-2}, and the corresponding power density can reach 0.9 mW cm^{-2}. The increase in voltage is related to their charge storage mechanism. During the charging, Zn^{2+} first extracts from the cathode due to strong electrostatic interaction. Then, H$^+$ is released from the carbonyl group of poly(4,40-TDP). This continuous extraction leads to a wide voltage window of the device. The interfacial redox reaction is also a viable strategy for increasing the energy density of the device.

Ramanujam's group [98] synthesized a porous AC from chitosan and N, N′-bis(glycinyl) naphthalene diimide (H_2BNDI) composite electrode material. The porous structure can reduce the transmission path of ions to facilitate the rapid transfer of ions. The presence of oxygen functional groups and N-enriched sites on the electrode surface can provide additional pseudocapacitance. Therefore, the fabricated devices deliver a specific capacitance of 500 F g^{-1} with an energy density of 250 Wh kg^{-1} at 0.1 A g^{-1}.

Graphene and CNT materials produce severe agglomeration and re-stacking. This significantly reduces their actual specific surface area and causes a reduction in the specific capacity. To address these drawbacks, it is necessary to fabricate composites with optimal structures. It is a common approach to prevent agglomeration by functionalizing graphene oxide with redox-active organic molecules. For example, Chen's group [99] introduced the p-phenylenediamine (PPD) into the interlayer of the graphene film. This enlarges the interlayer distance and exposes more ion-accessible regions. In addition, the partial reduction of the amino group improves the conductivity of the RGO film. Benefiting from the redox activity of PPD, the RGO@PPD film electrode shows high pseudocapacitance and EDLC for charge storage. Yang et al. [100] prepared a composite electrode of electrochemical graphene oxide (EGO) and polypyrrole (PPy) by one-step electrochemical co-deposition. The Zn-PPy/EGO hybrid capacitor obtains an energy density of 72.1 Wh kg^{-1} at 12.4 kW kg^{-1} and maintains the long-term cycle stability of 81% after 5000 cycles. Compared with chemical graphene oxide (CGO), EGO material possesses strong π-π interaction with PPy due to less structural destruction of graphene [101]. It is beneficial to enhance the conductivity of the composite material.

The lamination issue between 2D nanosheets can be effectively resolved by introducing additional dimensional materials, such as 1D carbon nanotubes [102,103]. Zhang and co-workers [104] developed kapok-derived N- and P-rich 2D thin-walled microporous carbon tiles (CTs). Leveraging the superior conductivity of single-walled carbon nanotubes (SWNTs), they constructed CT/SWNT porous paper cathodes with considerable specific surface area. The uniformly doped thin walled (~700 nm) structure can effectively shorten the ion diffusion path. The submicron layer spacing between the CTs with suitable curvature and carbon nanotubes builds a fast ion/charge transport channel. Based on this synergistic effect, this carbon cathode delivers a specific capacity of 127.6 mAh g^{-1} at 0.1 A g^{-1}. Even at 20 A g^{-1}, its specific capacity can still be kept at 72.4 mAh g^{-1}.

4.2. Morphology Regulation

The microstructure of carbon materials plays a pivotal role in regulating the electrochemical performance of energy storage devices. Carbon materials can be generally categorized into 0D carbon spheres, 1D carbon nanofibers, 2D carbon nanosheets, and 3D porous structures [30]. According to various preparation approaches, carbon spheres can be adjusted into hollow, yolk–shell, and core–shell structures. It possesses favorable conductivity and controllable particle size distribution. The hollow architecture facilitates the rapid transport of carriers and relieves the volume expansion in the long-term cycle [105].
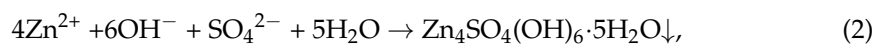
The template method is commonly utilized to prepare hollow structures. Yan's group [106] synthesized mesoporous hollow carbon spheres by the SiO_2 template method. They are used as cathodes and MCHSs-coated Zn foils as anodes to assemble hybrid capacitors in 2M $ZnSO_4$ electrolyte. The nanostructures of MCHSs electrodes provide abundant ion diffusion channels. In addition, the cladding layer inhibits the growth of dendrites/protrusions on the Zn anode surface. Based on the above advantages, the devices show a high energy density of 129.3 Wh kg^{-1} at 266.4 W kg^{-1} and a cycle retention of 96% after 10,000 cycles at 1 A g^{-1}. Further, they found that the capacity of the devices with different mass loadings decayed as the mass of the active substance increased. This is attributed to the sluggish ion and charge transport of thick electrodes. Nonetheless, the device can still achieve a specific capacity of 110 mAh g^{-1} at a high mass loading (20 mg cm^{-2}). Chen et al. [107] reported a copolymer-derived (polyaniline-co-polypyrrole) hollow carbon sphere using surfactant as a soft template. This cavity sphere possesses

a high surface area, which facilitates the increase of the active site of the electrode. The hollow structure expands the contact area between electrode and electrolyte. Therefore, the assembled capacitor shows an energy density of 59.7 Wh kg^{-1} and a power density of 447.8 W kg^{-1}. In addition, it can be stably cycled 15,000 times at 1 A g^{-1} with less capacity loss (2%).

4.3. Heteroatom Doping

Carbon materials doped with N, S, P, B, and other heteroatoms are increasingly gaining attention due to their high electron mobility and enhanced energy storage capacity [67,108,109]. The interaction between the heteroatoms and the host material improves the adsorption of electrolyte ions as well as optimizing the surface wettability and conductivity. This promotes rapid charge transfer, which effectively accelerates the point electrochemical kinetics. We mentioned above that the AC cathode suffers from a low practical specific capacity. In addition, it shows weak wettability at the interface with the electrolyte. This constrains the longevity of the device at high current densities [110]. Due to the formation of polar functional groups, the combination of N and O in carbon materials enhances the interaction with electrolytes, thus improving wettability. Wang et al. [111] reported that doping onion-like carbon with N and P elements significantly increased the surface area available for ion adsorption. The assembled N, P-OLC-based devices provide 63% capacity retention at 20 A g^{-1}. Their energy and power densities are 149.5 Wh kg^{-1} and 26.7 kW kg^{-1}. Among them, the doping of N significantly increases the hydrophilicity of the electrode interface, thus optimizing the contact resistance between the electrode and the electrolyte. Also, a nitric acid treatment can provide oxygen-containing functional groups on the surface of porous carbon, which contributes to the improvement of wettability [112]. Therefore, the device can obtain superior rate performance at high current density [113].

Dong's group [114] constructed a fiber-carbon cathode HPCF with a layered porous surface and O/N functional groups. The surface of the electrode contains a large number of micropores to provide high capacity, and the mesopores and macropores can ensure superior rate capability (Figure 9a). The CV curve further reveals that HPCF cathodes store more Zn^{2+} cations and SO$_4{}^{2-}$ anions at high scanning rates. This indicates that most of the stored charge of the cathode comes from SO$_4{}^{2-}$ anion storage. Figure 9b shows the capacitance contribution of the electrode gradually increases with the scanning rate. The reason could be that the rich N/O heteroatoms in HPCF cathode can enhance the interaction between pseudocapacitance behavior and electrolyte ions. The mechanism of charge storage is explored through combining various characterization methods. When the electrode is in the discharge state, Zn$_4$SO$_4$(OH)$_6\cdot$5H$_2$O flakes (BZS) appear. At charging, most of the flakes disappear. This may be due to the following reactions:

$$4Zn^{2+} + 6OH^- + SO_4{}^{2-} + 5H_2O \rightarrow Zn_4SO_4(OH)_6\cdot5H_2O\downarrow, \qquad (2)$$

In addition, the H+ provided by the acidic electrolyte adsorbs on the electrode surface, which results in an increase in the pH of the electrolyte. This suppresses the hydrogen evolution potential of the electrolyte. Only BZS products are detected in the structure of the HPCF cathode. This further confirms the energy storage mechanism of ion adsorption/desorption occurring at the surface of the electrode. Zheng et al. [69] designed an O-doped 3D porous carbon material. The combination of 3D porous structure and oxygen-containing functional group can endow the electrode with fast ion/electron transport and strong pseudocapacitance. The assembled flexible device can be recharged and discharged 10,000 times at 1.0 A g^{-1} with a capacity retention rate of 87.6%. Zhang's group [115] utilized potassium chloroacetate (ClCH$_2$COOK) as a carbon source and template to form oxygen-enriched porous carbon (ORCs) with an average pore size of 1.95–2.19 nm. This strategy can construct ORCs with high oxygen doping (4.38 atomic%). As a cathode material, it shows high EDLC and pseudocapacitance.

However, excessive oxygen functional groups can diminish the interaction between electrolyte ions and the carbon surface, which induces the aggravation of the self-discharge

behavior. This directly inhibits the dynamic process of the device [85]. Yuan et al. [116] modulated the temperature range during their hydrogen thermal reduction process to prepare superior starch-based porous carbon materials. It reveals the structural evolution of the reactive deoxygenation process. The results indicate that the pyrolysis and hydrogenation of oxygen functional groups may occur simultaneously. Among them, the HAC-700 electrode can be maintained for 10 h at an open-circuit voltage of 2.29 V, demonstrating strong resistance to self-discharge (Figure 9c). This may be associated with the suitable pore size in the carbon skeleton and the consumption of instable COOH and R-COOR groups. They can effectively improve the wettability of the electrode and prevent the electrolyte from irreversibly reacting with the unstable oxygen functional groups on the carbon electrode surface.

The addition of N can reduce the energy barrier of C-O interaction with Zn ions [117]. Lu's group [37] constructed capacitors with a lifetime of 100,000 cycles based on nitrogen-doped layered porous carbon (HNPC) as the cathode (Figure 9d). The existence of the N element optimizes the conductivity, electrochemical active surface area (ECSA) of the electrode, and surface wettability. It also improves the efficient transfer of ions/electrons and ensures sufficient storage space for charges. DFT calculation reveals the whole process of zinc ion adsorption and desorption. The adsorption of zinc ions causes the O-H bond to form a C-O-Zn bond, resulting in the release of H^+ ions. In Figure 9e, the reaction of an N-doped HNPC electrode only needs to overcome the energy barrier of 1.25 eV (2.13 eV for an undoped electrode). It effectively promotes the chemical adsorption of Zn ions on the electrode surface.

Biomass-derived porous carbon possesses inherent functional groups, or heteroatoms. It can offer sufficient active sites and surface wettability for the reaction. Therefore, the addition of chemical activators can further increase the specific surface area and optimize the pore structure, which is beneficial to the improvement of electrochemical performance. Wang et al. [118] proposed a novel potassium thioacetate activation technique. The pine needles are pyrolyzed as a carbon source to produce sulfur-doped 3D porous carbon (S-3DPCs). The prepared S-3DPCs material shows a specific surface area of 2336.9 m^2 g^{-1} and a certain amount of sulfur (0.88–3.60 at%). Therefore, the capacitor assembled with the S-3DPC-800 positive electrode can provide a specific capacity of 203.3 mAh g^{-1} (0.2 A g^{-1}) and 81 mAh g^{-1} (20 A g^{-1}). In addition, it can be recycled 18,000 times at 10 A g^{-1}, and the specific capacity retention reaches 96.8%.
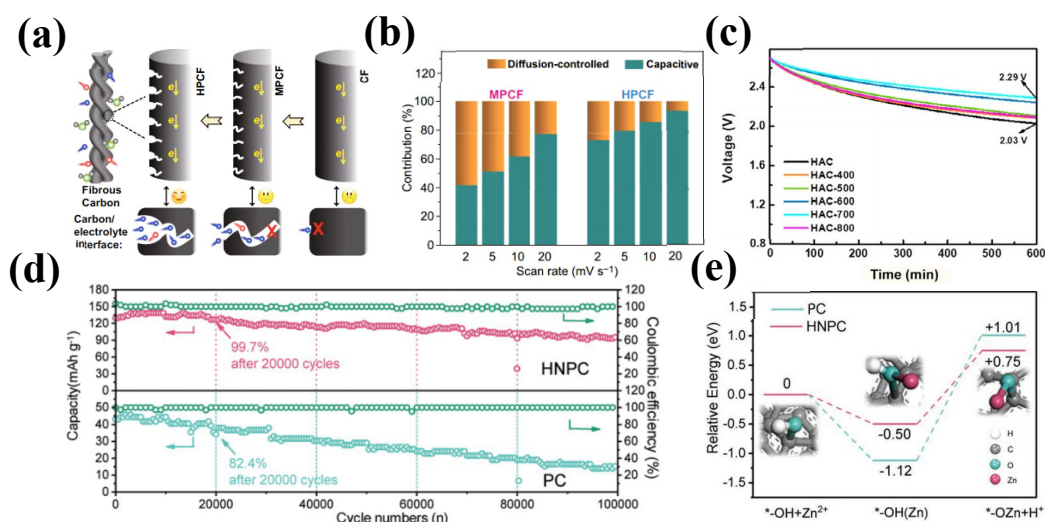

Figure 9. Performance of doped carbon-based materials. (**a**) Schematic of energy storage on cathodes with various surface conditions. (**b**) Contribution ratio of charge storage behavior. Reproduced with permission [114], Copyright 2021, Springer Nature. (**c**) Leakage current curves. Reproduced with permission [116], Copyright 2020, Elsevier B.V. and Science Press. (**d**) Cycling stability. (**e**) The energy profiles.* represents C atom. Reproduced with permission [37], Copyright 2019, Wiley-VCH.

Lu and his collaborators [119] designed the activation mechanism of microporous carbon (DSPCs) derived from sodium alginate through double templates. Highly active micropores (about 0.7–2.0 nm) endow the material with reasonable specific surface area and rich reaction sites. The assembled device shows an energy density of 99.22 Wh kg^{-1} (200 W kg^{-1}). The reversible specific capacity of the electrode is 87.5 mAh g^{-1} at 0.2 A g^{-1}. The capacity of 18.1 mAh g^{-1} can be maintained when the current density rises to 40 A g^{-1}.

In Table 1, we summarize the electrochemical performance of the various carbon-based electrodes. All of these electrode materials can achieve a long cycle life up to more than 10,000 cycles. Among them, the specific capacity of the hierarchical porous material is higher than that of the AC material. Oxygen-rich carbon electrodes can show a cycle life of more than 20,000 cycles. The atom-doped electrode materials demonstrate a long cycle life of up to 60,000 cycles with a capacity retention of 98.9% and a maximum power density of 48.8 kW kg^{-1}.

Table 1. The electrochemical performance of the various electrodes for ZIHCs.

Cathode	Electrolyte	Voltage (V)	Capacity/ Current Density (mAh g^{-1}/A g^{-1})	Capacity Retention/ Current Density/ The Long-Term Cycle (%/A g^{-1}/cycles)	Energy Density (Wh kg^{-1})	Power Density (kW kg^{-1})	Refs.
AC	2M ZnSO$_4$	0.2–1.8	121/0.1	91/10/10,000	30	14.9	[25]
O-rich porous carbon	3 M Zn(ClO$_4$)$_2$	0–1.9	179.8/0.1	99.2/20/30,000	40.4	48.8	[31]
Mesoporous AC	2M ZnSO$_4$	0.3–1.8	176/0.5	78/10/40,000	77	10.7	[66]
Porous AC	3M Zn(CF$_3$SO$_3$)$_2$	0.01–1.8	231/0.5	70/10/18,000	77.5	11.4	[80]
N doped pitch-derived carbon	1 M ZnSO$_4$	0–1.8	136.2/0.3	98.9/10/60,000	81.1	12.8	[81]
Porous carbon	1M Zn(CF$_3$SO$_3$)$_2$	0.2–1.8	183.7/0.2	92.2/10/10,000	65.4	15.7	[83]
O-rich porous carbon	2M ZnSO$_4$	0.2–1.8	317.8/0.5	91/10/20,000	136.3	20	[86]
O-enriched carbon fiber	gelatin/ZnSO$_4$ gel	0.2–1.8	136.4/0.1	81/5/50,000	97.7	9.9	[89]
3D graphene@PANI composite	2M ZnSO$_4$	0.3–1.6	154/0.1	80.5/5/6000	205	45.8	[93]
3D graphene	3M Zn(CF$_3$SO$_3$)$_2$	0.1–1.8	299 F cm^{-3}/0.1	85/5/30,000	61 Wh/L	23.2 kW/L	[94]
H$_2$BNDI@Ch-C	2 M ZnSO$_4$	0.1–1.9	500/0.1	80/5/10,000	55	9.5	[98]
PPy/EGO	1 M ZnCl$_2$	0.5–1.5	444.2/0.35	81/5 mA cm^{-2}/5000	72.1	12.4	[100]
Hollow carbon spheres	2M ZnSO$_4$	0.2–1.8	174.7/0.1	96/1/10,000	36.8	13.7	[106]
S-doped 3D porous carbon	2M ZnSO$_4$	0.2–1.8	203.3/0.2	96.8/10/18,000	64.8	16	[118]

5. Summary and Outlook

In summary, carbon-based materials are of interest owing to their structural diversity, superior electrical conductivity, and large specific surface area. These features render them crucial electrode materials in ZIHCs. We concentrate on the research advances of carbon cathode and discuss their energy storage mechanism, electrochemical performance, and electrode material structure optimization strategies. Some progress has been achieved, but there are still challenges in applications, especially in improving the energy power density and specific capacitance. At present, ZIHCs are in the infancy stage of growth, and more efforts are needed to propose new innovations to overcome these problems (Figure 10).

1. It is still difficult to identify the energy storage mechanism of ZIHCs. In the current study, carbon materials are often compounded with some materials for structural optimization in order to increase the specific capacity of electrodes. The pseudocapacitance during charge storage provides a partial contribution rather than simple ion adsorption/desorption. Furthermore, there is no complete clarification about the contribution ratio of the charge storage behavior. The combination of first-principles calculations, electrochemical kinetic analysis, and in situ structural characterization can also illustrate the structural changes of the electrode during charging and discharging and reveal the energy storage mechanism. The effect of by-product generation on electrode performance is still controversial.

2. Carbon-based electrode materials inherently show low specific capacitance and poor energy density. Suitable structural modifications, including heteroatom doping, microstructure modulation, and surface modification, can effectively improve the charge storage capacity of carbon-based materials. However, the constitutive relationship and intrinsic connection between structural improvement and electrochemical performance are still not clearly explained.

3. Commercially available zinc foils are usually the counter electrodes of the devices. Although they present high theoretical capacity, issues such as dendrite growth, corrosion, and HER reactions limit the high performance of ZIHCs. Therefore, it is essential to develop the structural design of anode materials to facilitate their advancement. For example, 3D nanostructured zinc electrodes possess rich active sites and a large electrolyte/electrode contact area. The uniformly distributed electric field can retard the growth of dendrites and promote the diffusion of ions.

4. Fully charged hybrid capacitors often suffer from spontaneous charge loss and voltage drop, resulting in self-discharge. The existence of the self-discharge process limits its market application. For carbon-based electrodes, ash and oxygen-containing functional groups can weaken the interaction between electrolyte ions and the electrode surface and enhance the self-discharge rate. In addition, the pore effect of porous structures leads to the redistribution of charges in carbon materials. We should also focus on the self-discharge behavior of devices in diverse working conditions. The corresponding approach is established to suppress the self-discharge of the device.
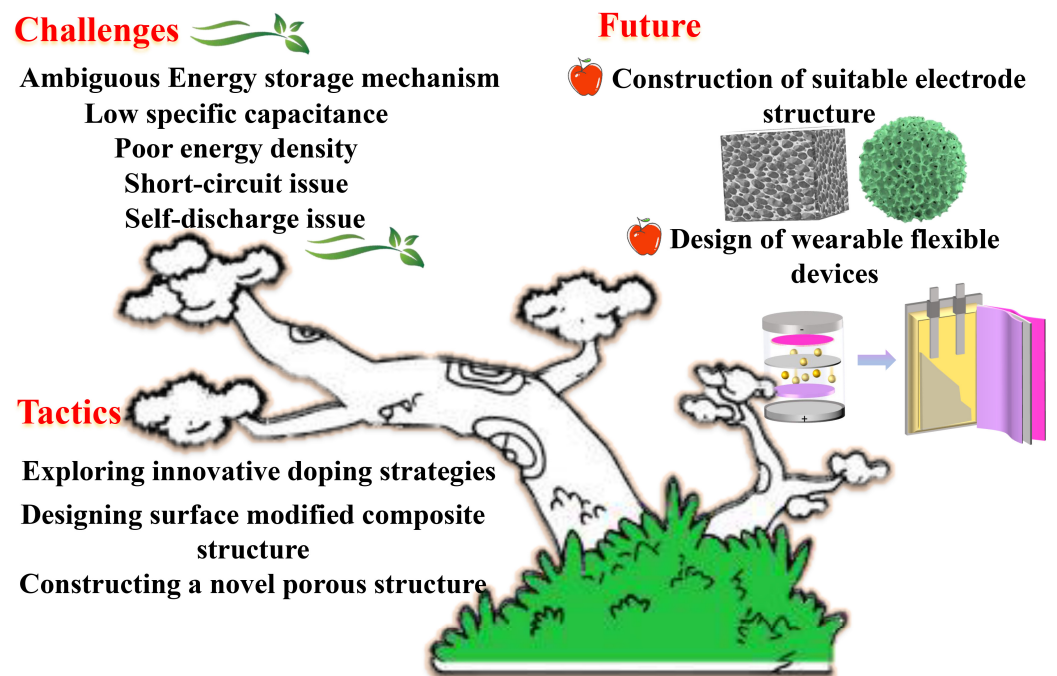

Figure 10. Challenges, tactics, and future goals for carbon-based electrodes of ZIHCs.

In the future, we consider that ZIHCs should concern the following aspects:

1. It is necessary to explore novel electrode material synthesis tactics to obtain porous carbon with favorable pore size and electrolyte ion compatibility. Various carbon-based precursor materials, such as biomass, asphalt, and polymers, possess diverse physical and chemical properties. It is helpful to design reasonable approaches according to their properties to give full play to the characteristics of raw materials and avoid their shortcomings.

2. The development of gel electrolyte is in line with the future development trend. Ordinary diaphragm is easy to be pierced by zinc branches in long-term circulation, resulting in a short circuit. Hydrogel electrolyte shows certain flexibility and mechanical strength, which can effectively slow down the growth of zinc dendrites. In addition, with the development of wearable flexible devices, positive and negative electrodes as well as the matching of the diaphragm are a key concern. The electrodes of flexible capacitors need to meet the characteristics of superior mechanical flexibility, light weight, and high-pressure resistance. For instance, Wu's group [120] prepared a super-folded conductive carbon material based on the bionic design idea of silkworm

spinning–cocooning–reeling, which can withstand 1 million or even unlimited folds without any damage. These structural materials possess superior mechanical properties. Their integration with ZIHCs can greatly improve the durability and life of devices. This synergy can promote the technological innovation of wearable devices.

3. Combining advanced in situ characterization techniques, it allows an intensive investigation into the structure of the electrodes and the dynamic changes in the energy storage process. It is essential for revealing the electrode energy storage process. Also, the structural design of electrode materials combined with theoretical calculation can provide theoretical guidance for structural stability, reaction-free energy, ion adsorption, diffusion, and reaction processes.

Author Contributions: Conceptualization, investigation, and resources, Y.L., L.S. and C.L.; writing—original draft preparation, Y.L. and C.S.; writing—review and editing, Y.L., C.S., L.S., C.L. and X.W.; visualization, Y.L. and C.S.; supervision, Y.L. and X.W. All authors have read and agreed to the published version of the manuscript.

Data Availability Statement: All data used for this work are included within the manuscript.

Conflicts of Interest: Authors Ying Liu, Lechun Song, Chenze Li and Caicheng Song were employed by the company SINOPEC Dalian (Fushun) Research Institute of Petroleum and Petrochemicals. The remaining author declare that the research was conducted in the absence of any commercial or financial relationships that could be construed as a potential conflict of interest.

References

1. Huang, Y.; Zhu, M.; Huang, Y.; Pei, Z.; Li, H.; Wang, Z.; Xue, Q.; Zhi, C. Multifunctional Energy Storage and Conversion Devices. *Adv. Mater.* **2016**, *28*, 8344–8364. [CrossRef] [PubMed]

2. Zheng, M.; Tang, H.; Hu, Q.; Zheng, S.; Li, L.; Xu, J.; Pang, H. Tungsten-Based Materials for Lithium-Ion Batteries. *Adv. Funct. Mater.* **2018**, *28*, 1707500. [CrossRef]

3. Ue, M.; Sakaushi, K.; Uosaki, K. Basic knowledge in battery research bridging the gap between academia and industry. *Mater. Horiz.* **2020**, *7*, 1937–1954. [CrossRef]

4. Wang, H.; Zhu, C.; Chao, D.; Yan, Q.; Fan, H.J. Nonaqueous Hybrid Lithium-Ion and Sodium-Ion Capacitors. *Adv. Mater.* **2017**, *29*, 1702093. [CrossRef] [PubMed]

5. Dong, L.; Yang, W.; Yang, W.; Li, Y.; Wu, W.; Wang, G. Multivalent metal ion hybrid capacitors: A review with a focus on zinc-ion hybrid capacitors. *J. Mater. Chem. A* **2019**, *7*, 13810–13832. [CrossRef]

6. Liu, H.; Zhao, D.; Hu, P.; Wu, X. Ternary core-shell structured transition metal chalcogenide for hybrid electrochemical capacitor. *Chin. Chem. Lett.* **2018**, *29*, 1799–1803. [CrossRef]

7. Yang, Y.; Yang, S.; Xue, X.; Zhang, X.; Li, Q.; Yao, Y.; Rui, X.; Pan, H.; Yu, Y. Inorganic All-Solid-State Sodium Batteries: Electrolyte Designing and Interface Engineering. *Adv. Mater.* **2024**, *36*, 2308332. [CrossRef]

8. Sun, J.; Zhang, Q.; Liu, C.; Zhang, A.; Hou, L.; Yuan, C. Conductive Zinc-Based Metal–Organic Framework Nanorods as Cathodes for High-Performance Zn-Ion Capacitors. *Batteries* **2024**, *10*, 222. [CrossRef]

9. Zhou, J.; Hu, H.-Y.; Li, H.-Q.; Chen, Z.-P.; Yuan, C.-Z.; He, X.-J. Advanced carbon-based materials for Na, K, and Zn ion hybrid capacitors. *Rare Met.* **2023**, *42*, 719–739. [CrossRef]

10. Liu, Y.; Liu, Y.; Wu, X.; Cho, Y.-R. Enhanced Electrochemical Performance of Zn/VO$_x$ Batteries by a Carbon-Encapsulation Strategy. *ACS Appl. Mater. Interfaces* **2022**, *14*, 11654–11662. [CrossRef]

11. Zhao, D.; Wang, X.; Zhang, W.; Zhang, Y.; Lei, Y.; Huang, X.; Zhu, Q.; Liu, J. Unlocking the Capacity of Vanadium Oxide by Atomically Thin Graphene-Analogous V$_2$O$_5$·nH$_2$O in Aqueous Zinc-Ion Batteries. *Adv. Funct. Mater.* **2023**, *33*, 2211412. [CrossRef]

12. Liu, Y.; Liu, Y.; Wu, X. Rational design of bi-phase CaV$_2$O$_6$/NaV$_6$O$_{15}$ cathode materials for long-life aqueous zinc batteries. *EcoMat* **2023**, *5*, e12409. [CrossRef]

13. Blanc, L.E.; Kundu, D.; Nazar, L.F. Scientific Challenges for the Implementation of Zn-Ion Batteries. *Joule* **2020**, *4*, 771–799. [CrossRef]

14. Liu, Y.; Wu, X. Review of vanadium-based electrode materials for rechargeable aqueous zinc ion batteries. *J. Energy Chem.* **2021**, *56*, 223–237. [CrossRef]

15. Tang, B.; Shan, L.; Liang, S.; Zhou, J. Issues and opportunities facing aqueous zinc-ion batteries. *Energy Environ. Sci.* **2019**, *12*, 3288–3304. [CrossRef]

16. Liu, Y.; Wu, X. High durable aqueous zinc ion batteries by synergistic effect of V_6O_{13}/VO_2 electrode materials. *J. Energy Chem.* **2023**, *87*, 334–341. [CrossRef]

17. Sun, Y.; Liu, B.; Liu, L.; Lang, J.; Qiu, J. A Low-Concentration and High Ionic Conductivity Aqueous Electrolyte toward Ultralow-Temperature Zinc-Ion Hybrid Capacitors. *Small Struct.* **2023**, *4*, 2200345. [CrossRef]

18. Liu, Y.; Zhao, D.; Liu, H.; Umar, A.; Wu, X. High performance hybrid supercapacitor based on hierarchical MoS_2/Ni_3S_2 metal chalcogenide. *Chin. Chem. Lett.* **2019**, *30*, 1105–1110. [CrossRef]

19. Muzaffar, A.; Ahamed, M.B.; Deshmukh, K.; Thirumalai, J. A review on recent advances in hybrid supercapacitors: Design, fabrication and applications. *Renew. Sust. Energy Rev.* **2019**, *101*, 123–145. [CrossRef]

20. Liu, Y.; Umar, A.; Wu, X. Metal-organic framework derived porous cathode materials for hybrid zinc ion capacitor. *Rare Met.* **2022**, *41*, 2985–2991. [CrossRef]

21. Yu, L.; Li, J.; Ahmad, N.; He, X.; Wan, G.; Liu, R.; Ma, X.; Liang, J.; Jiang, Z.; Zhang, G. Recent progress on carbon materials for emerging zinc-ion hybrid capacitors. *J. Mater. Chem. A* **2024**, *12*, 9400–9420. [CrossRef]

22. Miao, L.; Lv, Y.; Zhu, D.; Li, L.; Gan, L.; Liu, M. Recent advances in zinc-ion hybrid energy storage: Coloring high-power capacitors with battery-level energy. *Chin. Chem. Lett.* **2023**, *34*, 107784. [CrossRef]

23. Lal, M.S.; Arjunan, A.; Balasubramanian, V.; Sundara, R. Redox-active polymer hydrogel electrolyte in biowaste-derived microporous carbon-based high capacitance and energy density ultracapacitors. *J. Electroanal. Chem.* **2020**, *870*, 114236. [CrossRef]

24. Tian, Y.; Amal, R.; Wang, D.-W. An Aqueous Metal-Ion Capacitor with Oxidized Carbon Nanotubes and Metallic Zinc Electrodes. *Front. Energy Res.* **2016**, *4*, 34. [CrossRef]

25. Dong, L.; Ma, X.; Li, Y.; Zhao, L.; Liu, W.; Cheng, J.; Xu, C.; Li, B.; Yang, Q.H.; Kang, F. Extremely safe, high-rate and ultralong-life zinc-ion hybrid supercapacitors. *Energy Storage Mater.* **2018**, *13*, 96–102. [CrossRef]

26. Li, Z.; An, Y.; Dong, S.; Chen, C.; Wu, L.; Sun, Y.; Zhang, X. Progress on zinc ion hybrid supercapacitors: Insights and challenges. *Energy Storage Mater.* **2020**, *31*, 252–266. [CrossRef]

27. Ma, X.; Cheng, J.; Dong, L.; Liu, W.; Mou, J.; Zhao, L.; Wang, J.; Ren, D.; Wu, J.; Xu, C.; et al. Multivalent ion storage towards high-performance aqueous zinc-ion hybrid supercapacitors. *Energy Storage Mater.* **2019**, *20*, 335–342. [CrossRef]

28. Sun, Y.; Shi, X.L.; Yang, Y.L.; Suo, G.Q.; Zhang, L.; Lu, S.Y.; Chen, Z.G. Biomass-Derived Carbon for High-Performance Batteries: From Structure to Properties. *Adv. Funct. Mater.* **2022**, *32*, 2201584. [CrossRef]

29. Li, X.; Wei, B.Q. Supercapacitors based on nanostructured carbon. *Nano Energy* **2013**, *2*, 159–173. [CrossRef]

30. Liu, Y.; Wu, L. Recent advances of cathode materials for zinc-ion hybrid capacitors. *Nano Energy* **2023**, *109*, 108290. [CrossRef]

31. Yin, J.; Zhang, W.; Wang, W.; Alhebshi, N.A.; Salah, N.; Alshareef, H.N. Electrochemical Zinc Ion Capacitors Enhanced by Redox Reactions of Porous Carbon Cathodes. *Adv. Energy Mater.* **2020**, *10*, 2001705. [CrossRef]

32. Fan, X.; Liu, P.; Ouyang, B.; Cai, R.; Chen, X.; Liu, X.; Liu, W.; Wang, J.; Liu, K. Polyacrylonitrile Derived Porous Carbon for Zinc-Ion Hybrid Capacitors with High Energy Density. *ChemElectroChem* **2021**, *8*, 3572–3578. [CrossRef]

33. Li, Y.; Lu, P.; Shang, P.; Wu, L.; Wang, X.; Dong, Y.; He, R.; Wu, Z.-S. Pyridinic nitrogen enriched porous carbon derived from bimetal organic frameworks for high capacity zinc ion hybrid capacitors with remarkable rate capability. *J. Energy Chem.* **2021**, *56*, 404–411. [CrossRef]

34. Huang, Z.; Wang, T.; Song, H.; Li, X.; Liang, G.; Wang, D.; Yang, Q.; Chen, Z.; Ma, L.; Liu, Z.; et al. Effects of Anion Carriers on Capacitance and Self-Discharge Behaviors of Zinc Ion Capacitors. *Angew. Chem. Int. Ed.* **2020**, *60*, 1011–1021. [CrossRef]

35. Kühnel, R.-S.; Reber, D.; Battaglia, C. A High-Voltage Aqueous Electrolyte for Sodium-Ion Batteries. *ACS Energy Lett.* **2017**, *2*, 2005–2006. [CrossRef]

36. Tan, J.; Liu, J. Electrolyte Engineering Toward High-Voltage Aqueous Energy Storage Devices. *Energy Environ. Mater.* **2020**, *4*, 302–306. [CrossRef]

37. Zhang, H.; Liu, Q.; Fang, Y.; Teng, C.; Liu, X.; Fang, P.; Tong, Y.; Lu, X. Boosting Zn-Ion Energy Storage Capability of Hierarchically Porous Carbon by Promoting Chemical Adsorption. *Adv. Mater.* **2019**, *31*, 1904948. [CrossRef]

38. Whittingham, M.S.; Siu, C.; Ding, J. Can Multielectron Intercalation Reactions Be the Basis of Next Generation Batteries? *Acc. Chem. Res.* **2018**, *51*, 258–264. [CrossRef]

39. Thomas, M.G.S.R.; Bruce, P.G.; Goodenough, J.B. Lithium Mobility in the Layered Oxide $Li_{1-x}COO_2$. *Solid State Ion.* **1985**, *17*, 13–19. [CrossRef]

40. Amatucci, G.G.; Badway, F.; Pasquier, A.D.; Zheng, T. An Asymmetric Hybrid Nonaqueous Energy Storage Cell. *J. Electrochem. Soc.* **2001**, *148*, A930. [CrossRef]

41. Raza, W.; Ali, F.; Raza, N.; Luo, Y.; Kim, K.-H.; Yang, J.; Kumar, S.; Mehmood, A.; Kwon, E.E. Recent advancements in supercapacitor technology. *Nano Energy* **2018**, *52*, 441–473. [CrossRef]

42. Simon, P.; Gogotsi, Y.; Dunn, B. Where Do Batteries End and Supercapacitors Begin? *Science* **2014**, *343*, 1210–1211. [CrossRef] [PubMed]

43. Zan, G.; Li, S.; Chen, P.; Dong, K.; Wu, Q.; Wu, T. Mesoporous Cubic Nanocages Assembled by Coupled Monolayers With 100% Theoretical Capacity and Robust Cycling. *ACS Cent. Sci.* **2024**, *10*, 1283–1294. [CrossRef] [PubMed]

44. Gui, Q.; Ba, D.; Li, L.; Liu, W.; Li, Y.; Liu, J. Recent advances in materials and device technologies for aqueous hybrid supercapacitors. *Sci. China Mater.* **2021**, *65*, 10–31. [CrossRef]

45. Zuo, W.; Li, R.; Zhou, C.; Li, Y.; Xia, J.; Liu, J. Battery-Supercapacitor Hybrid Devices: Recent Progress and Future Prospects. *Adv Sci* **2017**, *4*, 1600539. [CrossRef]

46. Wu, X.; Yao, S. Flexible electrode materials based on WO$_3$ nanotube bundles for high performance energy storage devices. *Nano Energy* **2017**, *42*, 143–150. [CrossRef]

47. Yan, J.; Wang, Q.; Wei, T.; Fan, Z. Recent Advances in Design and Fabrication of Electrochemical Supercapacitors with High Energy Densities. *Adv. Energy Mater.* **2014**, *4*, 1300816. [CrossRef]

48. Liu, C.; Wu, X.; Wang, B. Performance modulation of energy storage devices: A case of Ni-Co-S electrode materials. *Chem. Eng. J.* **2020**, *392*, 123651. [CrossRef]

49. Liu, H.; Dai, M.; Zhao, D.; Wu, X.; Wang, B. Realizing Superior Electrochemical Performance of Asymmetric Capacitors through Tailoring Electrode Architectures. *ACS Appl. Energy Mater.* **2020**, *3*, 7004–7010. [CrossRef]

50. Lv, Y.; Zhang, L.; Wei, X.; Qiu, B.; Zhang, W.; Qin, Q.; Jia, D.; He, X.; Liu, Z.; Wei, F. The emerging of zinc-ion hybrid supercapacitors: Advances, challenges, and future perspectives. *Sustain. Mater. Technol.* **2023**, *35*, e00536. [CrossRef]

51. Wang, Y.; Sun, S.; Wu, X.; Liang, H.; Zhang, W. Status and Opportunities of Zinc Ion Hybrid Capacitors: Focus on Carbon Materials, Current Collectors, and Separators. *Nano Micro Lett.* **2023**, *15*, 78. [CrossRef] [PubMed]

52. Sui, D.; Wu, M.; Shi, K.; Li, C.; Lang, J.; Yang, Y.; Zhang, X.; Yan, X.; Chen, Y. Recent progress of cathode materials for aqueous zinc-ion capacitors: Carbon-based materials and beyond. *Carbon* **2021**, *185*, 126–151. [CrossRef]

53. Liu, Z.; Duan, C.; Dou, S.; Yuan, Q.; Xu, J.; Liu, W.D.; Chen, Y. Ultrafast Porous Carbon Activation Promises High-Energy Density Supercapacitors. *Small* **2022**, *18*, 2200954. [CrossRef] [PubMed]

54. Selvaraj, A.R.; Muthusamy, A.; Inho, C.; Kim, H.-J.; Senthil, K.; Prabakar, K. Ultrahigh surface area biomass derived 3D hierarchical porous carbon nanosheet electrodes for high energy density supercapacitors. *Carbon* **2021**, *174*, 463–474. [CrossRef]

55. Liu, Y.; Liu, Y.; Wu, X.; Cho, Y.-R. General Carbon Modification Avenue to Construct Highly Stable V$_2$O$_5$ Electrodes for Aqueous Zinc-Ion Batteries. *ACS Sustain. Chem. Eng.* **2023**, *11*, 13298–13305. [CrossRef]

56. Jin, J.; Geng, X.; Chen, Q.; Ren, T.-L. A Better Zn-Ion Storage Device: Recent Progress for Zn-Ion Hybrid Supercapacitors. *Nano Micro Lett.* **2022**, *14*, 64. [CrossRef]

57. Pomerantseva, E.; Bonaccorso, F.; Feng, X.; Cui, Y.; Gogotsi, Y. Energy storage: The future enabled by nanomaterials. *Science* **2019**, *366*, eaan8285. [CrossRef]

58. Borchardt, L.; Leistenschneider, D.; Haase, J.; Dvoyashkin, M. Revising the Concept of Pore Hierarchy for Ionic Transport in Carbon Materials for Supercapacitors. *Adv. Energy Mater.* **2018**, *8*, 1800892. [CrossRef]

59. Lee, J.; Kim, J.; Hyeon, T. Recent Progress in the Synthesis of Porous Carbon Materials. *Adv. Mater.* **2006**, *18*, 2073–2094. [CrossRef]

60. Presser, V.; Heon, M.; Gogotsi, Y. Carbide-Derived Carbons-From Porous Networks to Nanotubes and Graphene. *Adv. Funct. Mater.* **2011**, *21*, 810–833. [CrossRef]

61. Borchardt, L.; Oschatz, M.; Kaskel, S. Tailoring porosity in carbon materials for supercapacitor applications. *Mater. Horiz.* **2014**, *1*, 157–168. [CrossRef]

62. Wang, C.; Pei, Z.; Meng, Q.; Zhang, C.; Sui, X.; Yuan, Z.; Wang, S.; Chen, Y. Toward Flexible Zinc-Ion Hybrid Capacitors with Superhigh Energy Density and Ultralong Cycling Life: The Pivotal Role of ZnCl$_2$ Salt-Based Electrolytes. *Angew. Chem. Int. Ed.* **2020**, *60*, 990–997. [CrossRef] [PubMed]

63. Lv, K.; Zhang, J.; Zhao, X.; Kong, N.; Tao, J.; Zhou, J. Understanding the Effect of Pore Size on Electrochemical Capacitive Performance of MXene Foams. *Small* **2022**, *18*, 2202203. [CrossRef] [PubMed]

64. Jian, W.; Zhang, W.; Wei, X.; Wu, B.; Liang, W.; Wu, Y.; Yin, J.; Lu, K.; Chen, Y.; Alshareef, H.N.; et al. Engineering Pore Nanostructure of Carbon Cathodes for Zinc Ion Hybrid Supercapacitors. *Adv. Funct. Mater.* **2022**, *32*, 2209914. [CrossRef]

65. Hulicova Jurcakova, D.; Seredych, M.; Lu, G.Q.; Bandosz, T.J. Combined Effect of Nitrogen- and Oxygen-Containing Functional Groups of Microporous Activated Carbon on its Electrochemical Performance in Supercapacitors. *Adv. Funct. Mater.* **2009**, *19*, 438–447. [CrossRef]

66. An, G.H. Ultrafast long-life zinc-ion hybrid supercapacitors constructed from mesoporous structured activated carbon. *Appl. Surf. Sci.* **2020**, *530*, 147220. [CrossRef]

67. Liu, Y.; Liu, Y.; Wu, X. Defect engineering of vanadium-based electrode materials for zinc ion battery. *Chin. Chem. Lett.* **2023**, *34*, 107839. [CrossRef]

68. Song, C.; Liu, K.; Wang, T.; Zhao, P.-Y.; Huang, H.; Liu, Y.; Lu, R.; Zhang, S. Spontaneous template approach towards nitrogenous multi-shelled hollow carbon spheres with unique onion-like architecture. *Mater. Today Chem.* **2024**, *40*, 102196. [CrossRef]

69. Zheng, Y.; Zhao, W.; Jia, D.; Liu, Y.; Cui, L.; Wei, D.; Zheng, R.; Liu, J. Porous carbon prepared via combustion and acid treatment as flexible zinc-ion capacitor electrode material. *Chem. Eng. J.* **2020**, *387*, 124161. [CrossRef]

70. Zhang, Y.; Wang, Z.; Li, D.; Sun, Q.; Lai, K.; Li, K.; Yuan, Q.; Liu, X.; Ci, L. Ultrathin carbon nanosheets for highly efficient capacitive K-ion and Zn-ion storage. *J. Mater. Chem. A* **2020**, *8*, 22874–22885. [CrossRef]

71. Deng, S.; Yuan, Z.; Tie, Z.; Wang, C.; Song, L.; Niu, Z. Electrochemically Induced MOF-Derived Amorphous V$_2$O$_5$ for Superior Rate Aqueous Zn-Ion Batteries. *Angew Chem. Int. Ed.* **2020**, *59*, 22002. [CrossRef] [PubMed]

72. Li, H.; Liao, Q.; Liu, Y.; Li, Y.; Niu, X.; Zhang, D.; Wang, K. Hierarchically Porous Carbon Rods Derived from Metal-Organic Frameworks for Aqueous Zinc-Ion Hybrid Capacitors. *Small* **2023**, *20*, 2307184. [CrossRef] [PubMed]

73. Wang, H.; Shao, Y.; Mei, S.; Lu, Y.; Zhang, M.; Sun, J.-k.; Matyjaszewski, K.; Antonietti, M.; Yuan, J. Polymer-Derived Heteroatom-Doped Porous Carbon Materials. *Chem. Rev.* **2020**, *120*, 9363–9419. [CrossRef] [PubMed]

74. Yang, S.-H.; Fu, W.-Q.; Cui, Y.-W.; Cao, B.-Q. PVP/PAN-derived porous carbon fiber for zinc-ion hybrid supercapacitors. *Rare Met.* **2024**, *43*, 3066–3073. [CrossRef]

75. Zhang, Y.; Wang, L.; Jia, D.; Yue, L.; Zhang, H.; Liu, J. Hierarchical Porous Doped Carbon Plates Derived from Chitosan Aerogel as Cathode for High Performance Zn-ion Hybrid Capacitor. *ChemElectroChem* **2023**, *10*, e202200972. [CrossRef]

76. Pan, L.; Wang, Y.; Hu, H.; Li, X.; Liu, J.; Guan, L.; Tian, W.; Wang, X.; Li, Y.; Wu, M. 3D self-assembly synthesis of hierarchical porous carbon from petroleum asphalt for supercapacitors. *Carbon* **2018**, *134*, 345–353. [CrossRef]

77. Zhang, M.; Sun, Z.; Zhang, T.; Qin, B.; Sui, D.; Xie, Y.; Ma, Y.; Chen, Y. Porous asphalt/graphene composite for supercapacitors with high energy density at superior power density without added conducting materials. *J. Mater. Chem. A* **2017**, *5*, 21757–21764. [CrossRef]

78. Zhang, X.; Tian, X.; Song, Y.; Wu, J.; Yang, T.; Liu, Z. Boosting Zn-ion storage capacity of pitch coke-based activated carbon via pre-oxidation assisted KOH activation strategy. *Micropor. Mesopor. Mater.* **2022**, *333*, 111721. [CrossRef]

79. Yang, Y.; Li, Z.; Zhao, J.; Qu, S. Structural engineering of pitch-based porous carbon and its application in supercapacitors: A review. *J. Energy Storage* **2023**, *74*, 109334. [CrossRef]

80. Zhou, Z.; Zhou, X.; Zhang, M.; Mu, S.; Liu, Q.; Tang, Y. In Situ Two-Step Activation Strategy Boosting Hierarchical Porous Carbon Cathode for an Aqueous Zn-Based Hybrid Energy Storage Device with High Capacity and Ultra-Long Cycling Life. *Small* **2020**, *16*, 2003174. [CrossRef]

81. Shi, X.; Zhang, H.; Zeng, S.; Wang, J.; Cao, X.; Liu, X.; Lu, X. Pyrrolic-Dominated Nitrogen Redox Enhances Reaction Kinetics of Pitch-Derived Carbon Materials in Aqueous Zinc Ion Hybrid Supercapacitors. *ACS Mater. Lett.* **2021**, *3*, 1291–1299. [CrossRef]

82. Saini, S.; Chand, P.; Joshi, A. Biomass derived carbon for supercapacitor applications: Review. *J. Energy Storage* **2021**, *39*, 102646. [CrossRef]

83. Li, Z.; Chen, D.; An, Y.; Chen, C.; Wu, L.; Chen, Z.; Sun, Y.; Zhang, X. Flexible and anti-freezing quasi-solid-state zinc ion hybrid supercapacitors based on pencil shavings derived porous carbon. *Energy Storage Mater.* **2020**, *28*, 307–314. [CrossRef]

84. Zhao, L.; Jian, W.; Zhang, X.; Wen, F.; Zhu, J.; Huang, S.; Yin, J.; Lu, K.; Zhou, M.; Zhang, W.; et al. Multi-scale self-templating synthesis strategy of lignin-derived hierarchical porous carbons toward high-performance zinc ion hybrid supercapacitors. *J. Energy Storage* **2022**, *53*, 105095. [CrossRef]

85. Liu, K.; Yu, C.; Guo, W.; Ni, L.; Yu, J.; Xie, Y.; Wang, Z.; Ren, Y.; Qiu, J. Recent research advances of self-discharge in supercapacitors: Mechanisms and suppressing strategies. *J. Energy Chem.* **2021**, *58*, 94–109. [CrossRef]

86. Li, H.; Su, P.; Liao, Q.; Liu, Y.; Li, Y.; Niu, X.; Liu, X.; Wang, K. Olive Leaves-Derived Hierarchical Porous Carbon as Cathode Material for Anti-Self-Discharge Zinc-Ion Hybrid Capacitor. *Small* **2023**, *19*, 2304172. [CrossRef]

87. He, H.; Lian, J.; Chen, C.; Xiong, Q.; Zhang, M. Super hydrophilic carbon fiber film for freestanding and flexible cathodes of zinc-ion hybrid supercapacitors. *Chem. Eng. J.* **2021**, *421*, 129786. [CrossRef]

88. Li, Z.; Gadipelli, S.; Li, H.; Howard, C.A.; Brett, D.J.L.; Shearing, P.R.; Guo, Z.; Parkin, I.P.; Li, F. Tuning the interlayer spacing of graphene laminate films for efficient pore utilization towards compact capacitive energy storage. *Nat. Energy* **2020**, *5*, 160–168. [CrossRef]

89. Hu, X.; Bao, X.; Zhang, M.; Fang, S.; Liu, K.; Wang, J.; Liu, R.; Kim, S.H.; Baughman, R.H.; Ding, J. Recent Advances in Carbon Nanotube-Based Energy Harvesting Technologies. *Adv. Mater.* **2023**, *35*, 2303035. [CrossRef]

90. Wei, F.; Wei, Y.; Wang, J.; Han, M.; Lv, Y. N, P dual doped foamy-like carbons with abundant defect sites for zinc ion hybrid capacitors. *Chem. Eng. J.* **2022**, *450*, 137919. [CrossRef]

91. Sun, Y.; Zheng, J.; Tong, Y.; Wu, Y.; Liu, X.; Niu, L.; Li, H. Construction of three-dimensional nitrogen doped porous carbon flake electrodes for advanced potassium-ion hybrid capacitors. *J. Colloid Interface Sci.* **2022**, *606*, 1940–1949. [CrossRef] [PubMed]

92. Fang, X.Y.; Yu, X.X.; Zheng, H.M.; Jin, H.B.; Wang, L.; Cao, M.S. Temperature- and thickness-dependent electrical conductivity of few-layer graphene and graphene nanosheets. *Phys. Lett. A* **2015**, *379*, 2245–2251. [CrossRef]

93. Han, J.; Wang, K.; Liu, W.; Li, C.; Sun, X.; Zhang, X.; An, Y.; Yi, S.; Ma, Y. Rational design of nano-architecture composite hydrogel electrode towards high performance Zn-ion hybrid cell. *Nanoscale* **2018**, *10*, 13083–13091. [CrossRef] [PubMed]

94. Xu, X.; Zhao, X.; Yang, Z.; Lin, Q.; Jian, B.; Li, N.; Zheng, C.; Lv, W. High-density three-dimensional graphene cathode with a tailored pore structure for high volumetric capacity zinc-ion storage. *Carbon* **2022**, *186*, 624–631. [CrossRef]

95. Mao, J.; Iocozzia, J.; Huang, J.; Meng, K.; Lai, Y.; Lin, Z. Graphene aerogels for efficient energy storage and conversion. *Energy Environ. Sci.* **2018**, *11*, 772–799. [CrossRef]

96. Okhay, O.; Tkach, A.; Gallo, M.J.H.; Otero-Irurueta, G.; Mikhalev, S.; Staiti, P.; Lufrano, F. Energy storage of supercapacitor electrodes on carbon cloth enhanced by graphene oxide aerogel reducing conditions. *J. Energy Storage* **2020**, *32*, 101839. [CrossRef]

97. Xin, T.; Wang, Y.; Wang, N.; Zhao, Y.; Li, H.; Zhang, Z.; Liu, J. A high-capacity aqueous Zn-ion hybrid energy storage device using poly(4,4′-thiodiphenol)-modified activated carbon as a cathode material. *J. Mater. Chem. A* **2019**, *7*, 23076–23083. [CrossRef]

98. Potham, S.; Ramanujam, K. A novel hierarchical porous activated carbon-organic composite cathode material for high performance aqueous zinc-ion hybrid supercapacitors. *J. Power Sources* **2023**, *557*, 232551. [CrossRef]

99. Xu, Y.; Chen, X.; Huang, C.; Zhou, Y.; Fan, B.; Li, Y.; Hu, A.; Tang, Q.; Huang, K. Redox-active p-phenylenediamine functionalized reduced graphene oxide film through covalently grafting for ultrahigh areal capacitance Zn-ion hybrid supercapacitor. *J. Power Sources* **2021**, *488*, 229426. [CrossRef]

100. Yang, J.; Cao, J.; Peng, Y.; Bissett, M.; Kinloch, I.A.; Dryfe, R.A.W. Unlocking the energy storage potential of polypyrrole via electrochemical graphene oxide for high performance zinc-ion hybrid supercapacitors. *J. Power Sources* **2021**, *516*, 230663. [CrossRef]

101. Cao, J.; Wang, Y.; Chen, J.; Li, X.; Walsh, F.C.; Ouyang, J.H.; Jia, D.; Zhou, Y. Three-dimensional graphene oxide/polypyrrole composite electrodes fabricated by one-step electrodeposition for high performance supercapacitors. *J. Mater. Chem. A* **2015**, *3*, 14445–14457. [CrossRef]

102. Xu, T.; Yang, D.; Fan, Z.; Li, X.; Liu, Y.; Guo, C.; Zhang, M.; Yu, Z.-Z. Reduced graphene oxide/carbon nanotube hybrid fibers with narrowly distributed mesopores for flexible supercapacitors with high volumetric capacitances and satisfactory durability. *Carbon* **2019**, *152*, 134–143. [CrossRef]

103. Ni, T.; Wang, S.; Shi, J.; Du, X.; Cheng, Q.; Dong, Z.; Ruan, L.; Zeng, W.; Guo, X.; Ren, X.; et al. Highly Flexible and Self-Healable Zinc-Ion Hybrid Supercapacitors Based on MWCNTs-RGO Fibers. *Adv. Mater. Technol.* **2020**, *5*, 2000268. [CrossRef]

104. Cao, Y.; Tang, X.; Liu, M.; Zhang, Y.; Yang, T.; Yang, Z.; Yu, Y.; Li, Y.; Di, J.; Li, Q. Thin-walled porous carbon tile-packed paper for high-rate Zn-ion capacitor cathode. *Chem. Eng. J.* **2022**, *431*, 133241. [CrossRef]

105. Li, J.; Zhang, J.; Yu, L.; Gao, J.; He, X.; Liu, H.; Guo, Y.; Zhang, G. Dual-doped carbon hollow nanospheres achieve boosted pseudocapacitive energy storage for aqueous zinc ion hybrid capacitors. *Energy Storage Mater.* **2021**, *42*, 705–714. [CrossRef]

106. Liu, P.; Liu, W.; Huang, Y.; Li, P.; Yan, J.; Liu, K. Mesoporous hollow carbon spheres boosted, integrated high performance aqueous Zn-Ion energy storage. *Energy Storage Mater.* **2020**, *25*, 858–865. [CrossRef]

107. Chen, S.; Ma, L.; Zhang, K.; Kamruzzaman, M.; Zhi, C.; Zapien, J.A. A flexible solid-state zinc ion hybrid supercapacitors based on copolymer derived hollow carbon spheres. *J. Mater. Chem. A* **2019**, *7*, 7784–7790. [CrossRef]

108. Li, W.; Zhou, M.; Li, H.; Wang, K.; Cheng, S.; Jiang, K. A high performance sulfur-doped disordered carbon anode for sodium ion batteries. *Energy Environ. Sci.* **2015**, *8*, 2916–2921. [CrossRef]

109. Lee, Y.-G.; An, G.-H. Synergistic Effects of Phosphorus and Boron Co-Incorporated Activated Carbon for Ultrafast Zinc-Ion Hybrid Supercapacitors. *ACS Appl. Mater. Interfaces* **2020**, *12*, 41342–41349. [CrossRef]

110. Zhou, H.; Liu, C.; Wu, J.-C.; Liu, M.; Zhang, D.; Song, H.; Zhang, X.; Gao, H.; Yang, J.; Chen, D. Boosting the electrochemical performance through proton transfer for the Zn-ion hybrid supercapacitor with both ionic liquid and organic electrolytes. *J. Mater. Chem. A* **2019**, *7*, 9708–9715. [CrossRef]

111. Wang, H.; Chen, Q.; Xiao, P.; Cao, L. Unlocking Zinc-Ion Energy Storage Performance of Onion-Like Carbon by Promoting Heteroatom Doping Strategy. *ACS Appl. Mater. Interfaces* **2022**, *14*, 9013–9023. [CrossRef] [PubMed]

112. Nian, Y.-R.; Teng, H. Nitric Acid Modification of Activated Carbon Electrodes for Improvement of Electrochemical Capacitance. *J. Electrochem. Soc.* **2002**, *149*, A1008–A1014. [CrossRef]

113. Li, X.; Jiang, Y.; Wang, P.; Mo, Y.; Lai, W.; Li, Z.; Yu, R.; Du, Y.; Zhang, X.; Chen, Y. Effect of the oxygen functional groups of activated carbon on its electrochemical performance for supercapacitors. *New Carbon Mater.* **2020**, *35*, 232–243. [CrossRef]

114. Li, Y.; Yang, W.; Yang, W.; Wang, Z.; Rong, J.; Wang, G.; Xu, C.; Kang, F.; Dong, L. Towards High-Energy and Anti-Self-Discharge Zn-Ion Hybrid Supercapacitors with New Understanding of the Electrochemistry. *Nano Micro Lett.* **2021**, *13*, 95. [CrossRef] [PubMed]

115. Zhao, L.; Jian, W.; Zhu, J.; Zhang, X.; Wen, F.; Fei, X.; Chen, L.; Huang, S.; Yin, J.; Chodankar, N.R.; et al. Molten Salt Self-Template Synthesis Strategy of Oxygen-Rich Porous Carbon Cathodes for Zinc Ion Hybrid Capacitors. *ACS Appl. Mater. Interfaces* **2022**, *14*, 43431–43441. [CrossRef]

116. Yuan, S.; Huang, X.; Wang, H.; Xie, L.; Cheng, J.; Kong, Q.; Sun, G.; Chen, C.-M. Structure evolution of oxygen removal from porous carbon for optimizing supercapacitor performance. *J. Energy Chem.* **2020**, *51*, 396–404. [CrossRef]

117. Lou, G.; Pei, G.; Wu, Y.; Lu, Y.; Wu, Y.; Zhu, X.; Pang, Y.; Shen, Z.; Wu, Q.; Fu, S.; et al. Combustion conversion of wood to N, O co-doped 2D carbon nanosheets for zinc-ion hybrid supercapacitors. *Chem. Eng. J.* **2021**, *413*, 127502. [CrossRef]

118. Wang, D.; Wang, S.; Lu, Z. S-doped 3D porous carbons derived from potassium thioacetate activation strategy for zinc-ion hybrid supercapacitor applications. *Int. J. Energy Res.* **2020**, *45*, 2498–2510. [CrossRef]

119. Lu, Y.; Liu, L.; Zhang, R.; Jiang, Z.; Li, Y.; Sun, Z.; Chen, X.; Song, H. Sodium alginate-derived micropore dominated carbon 3D architectures through dual template engineering for high-performance Zn-ion hybrid capacitors. *Appl. Surf. Sci.* **2022**, *604*, 154631. [CrossRef]

120. Zan, G.; Wu, T.; Zhu, F.; He, P.; Cheng, Y.; Chai, S.; Wang, Y.; Huang, X.; Zhang, W.; Wan, Y.; et al. A biomimetic conductive super-foldable material. *Matter* **2021**, *4*, 3232–3247. [CrossRef]